

# Design, Synthesis, and Evaluation of a Novel Series of Indole Sulfonamide Peroxisome Proliferator Activated Receptor (PPAR) $\alpha/\gamma/\delta$ Triple Activators: Discovery of Lanifibranor, a New Antifibrotic Clinical Candidate

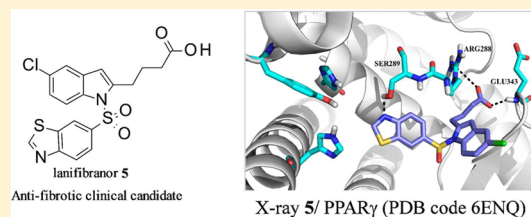
Benaïssa Boubia,<sup>\*,†,‡</sup> Olivia Poupardin,<sup>†</sup> Martine Barth,<sup>†</sup> Jean Binet,<sup>†</sup> Philippe Peralba,<sup>†</sup> Laurent Mounier,<sup>†</sup> Elise Jacquier,<sup>†</sup> Emilie Gauthier,<sup>†</sup> Valérie Lepais,<sup>†</sup> Maryline Chatar,<sup>†</sup> Stéphanie Ferry,<sup>‡</sup> Anne Thourigny,<sup>†</sup> Fabrice Guillier,<sup>†</sup> Jonathan Llacer,<sup>†</sup> Jérôme Amaudrut,<sup>†,‡</sup> Pierre Dodey,<sup>†</sup> Olivier Lacombe,<sup>†</sup> Philippe Masson,<sup>†</sup> Christian Montalbetti,<sup>†</sup> Guillaume Wettstein,<sup>†</sup> Jean-Michel Luccarini,<sup>†</sup> Christiane Legendre,<sup>†</sup> Jean-Louis Junien,<sup>†</sup> and Pierre Broqua<sup>†</sup>

<sup>†</sup>Inventiva, 50 rue de Dijon, 21121 Daix, France

<sup>‡</sup>Novalix, Boulevard Sebastien Brant Bioparc, 67405 Illkirch, France

## **S** Supporting Information

**ABSTRACT:** Here, we describe the identification and synthesis of novel indole sulfonamide derivatives that activate the three peroxisome proliferator activated receptor (PPAR) isoforms. Starting with a PPAR $\alpha$  activator, compound **4**, identified during a high throughput screening (HTS) of our proprietary screening library, a systematic optimization led to the discovery of lanifibranor (IVA337) **5**, a moderately potent and well balanced pan PPAR agonist with an excellent safety profile. In vitro and in vivo, compound **5** demonstrated strong activity in models that are relevant to nonalcoholic steatohepatitis (NASH) pathophysiology suggesting therapeutic potential for NASH patients.



## ■ INTRODUCTION

Nonalcoholic steatohepatitis (NASH) is a highly prevalent multifactorial and multistep disease associated with increasing risk of cardiovascular mortality and development of severe liver conditions such as cirrhosis and hepatocellular carcinoma.<sup>1,2</sup> NASH is characterized by histopathological changes in the liver, which include steatosis, inflammation, ballooning, necro-inflammation, and perisinusoidal fibrosis. Fibrosis stage is the strongest predictor for all-cause and disease-specific mortality in NASH patients.<sup>3</sup> Although the pathogenesis of NASH is not fully understood, there is a consensus that metabolic disorders and hepatic steatosis play a key role in the initiation of the disease.

Peroxisome proliferator activated receptors (PPARs) are members of the nuclear receptor family.<sup>4</sup> They play not only an important role in the regulation of lipid and glucose metabolism, but also in the regulation of inflammation and fibrogenesis.<sup>5,6</sup> Extensive efforts were deployed to identify potent and selective agonists, which could potentially be pharmacologically useful in metabolic diseases.<sup>7</sup> Two chemical families, thiazolidinediones represented by rosiglitazone **1a** and pioglitazone **1b** and fibrates represented by fenofibrate **2a** and bezafibrate **2b** (Figure 1), are well described in the literature as respectively glucose and lipid regulators.<sup>8–10</sup>

All three PPAR subtypes, PPAR $\alpha$  (NR1C1), PPAR $\delta$  (NR1C2), and PPAR $\gamma$  (NR1C3), are ligand-activated nuclear receptors, which exhibit isotype specific tissue expression and cellular

function.<sup>11,12</sup> The PPAR $\alpha$  isoform is highly expressed in hepatocytes, where it facilitates fatty acid transport beta-oxidation and dampens inflammatory response.<sup>13,14</sup> The PPAR $\delta$  isoform is found in most liver cells types (hepatocytes, hepatic stellate cells (HSC), and Kupffer cells) and contributes to the regulation of glucose and lipid metabolism while showing anti-inflammatory properties especially through the promotion of M2 stage Kupffer cells polarization.<sup>15,16</sup> The PPAR $\gamma$  isoform is highly expressed in the adipose tissue where it promotes adipocyte differentiation, increases glucose uptake, promotes storage of triglycerides, decreases plasma free fatty acids (FFA), and induces the secretion of the anti-inflammatory cytokine adiponectin. Activation of PPAR $\gamma$  increases insulin sensitivity of several organs including the liver.<sup>17,18</sup> Both PPAR $\gamma$  and PPAR $\delta$  are expressed at different extents in HSC, a primary cell driver of liver fibrosis. It is recognized that PPAR $\gamma$  plays a critical role in keeping HSC in a quiescent nonfibrogenic state.<sup>19,20</sup>

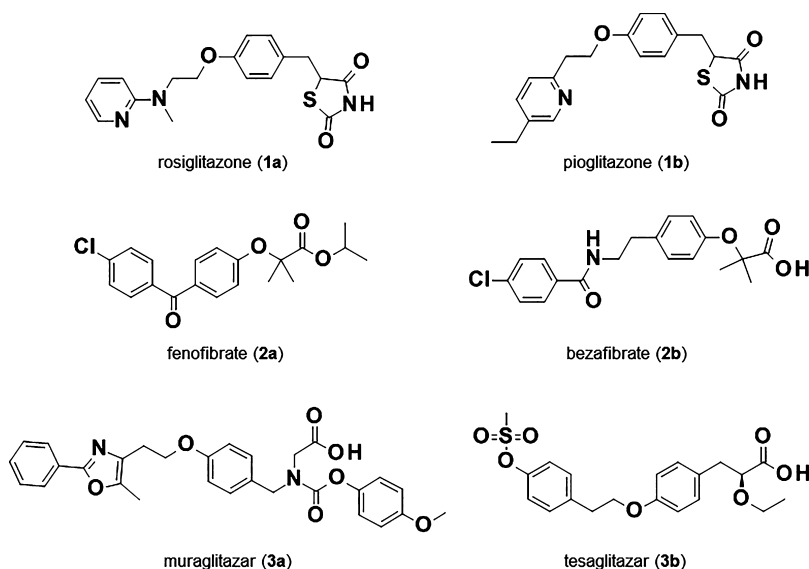
It can be speculated that combining PPAR $\alpha$ , PPAR $\delta$ , and PPAR $\gamma$  activation may bring an innovative and efficacious therapeutic approach to prevent the development and progression of NASH by addressing a large spectrum of parameters involved in the disease.

Many of the PPAR agonists that were developed and discontinued are very potent activators of the PPARs and

**Received:** September 1, 2017

**Published:** February 15, 2018





**Figure 1.** PPARs agonists. Compound 1a, rosiglitazone, and compound 1b, pioglitazone representing Thiazolidinedione family. Compound 2a, fenofibrate, and 2b, bezafibrate, representing Fibrate family. Compound 3a, muraglitazar, and 3b, tesaglitazar representing PPAR  $\alpha/\gamma$  dual agonists.

unbalanced relatively to the different isoforms targeted. This potentially could lead to a large spectrum of undesirable side effects as this strong potency would regulate the expression of a wide range of genes and activate many pathways, some of which will be associated with toxicity. Conversely, moderately potent PPAR agonists such as 2a, 2b, and 1b demonstrated good tolerability and safety in a large population of patients.<sup>21–23</sup> In our work, we chose to focus on moderately potent and well-balanced modulators of the three PPARs isoforms to target the NASH-related cells and pathways of interest while optimizing the therapeutic margin.

Our initial indole hit 4<sup>24</sup> was identified from a high throughput screening campaign of our proprietary compound collection using a human PPAR transactivation assays. This indole derivative showed a good agonist activity on PPAR $\alpha$  (half maximal effective concentration ( $EC_{50}$ ) = 260 nM, maximum efficacy ( $E_{max}$ ) = 101%) but an unbalanced pan PPAR profile with very low potency and efficacy on both PPAR $\delta$  ( $EC_{50}$  = 1912 nM,  $E_{max}$  = 56%) and PPAR $\gamma$  ( $EC_{50}$  = 1558 nM,  $E_{max}$  = 43%).

The structure of 4 offers similarities with the existing pharmacophoric scaffold, frequently described in PPAR agonist literature, which consists in an acidic headgroup that is attached to a hydrophobic tail group through a linker with various length and flexibility. As mentioned above, there is a clear unmet medical need in the therapeutic area of fibrotic disease like NASH. The objective of the optimization effort was the discovery of novel pan PPAR agonist drugs with an improved safety margin compared to the known PPAR $\gamma$  and dual PPAR $\alpha/\gamma$  compounds. This program led to the discovery of lanifibranor 5 (IVA337) 5 (Figure 2),<sup>24</sup> a moderately potent and well

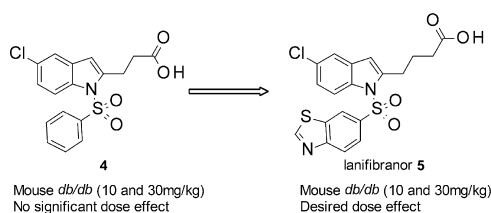
balanced pan PPAR agonist with an excellent safety profile, which is presently undergoing phase 2 clinical trials in NASH.

## RESULTS AND DISCUSSION

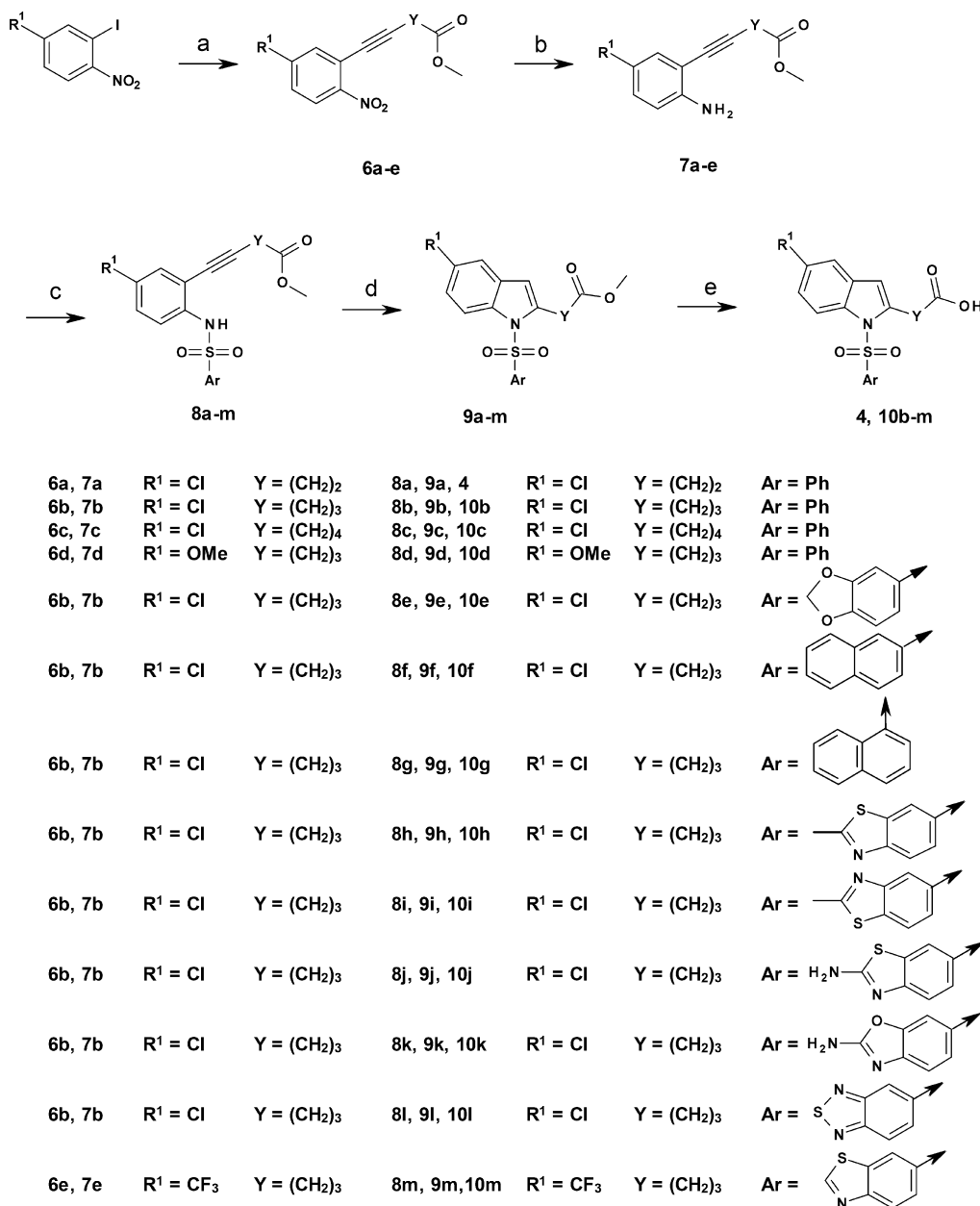
**Chemistry.** Synthetic routes to the indole compounds shown in Table 1–6 are outlined in Scheme 1–4. Palladium-catalyzed Sonogashira cross coupling between substituted iodo-nitrobenzenes and various alkynes afforded the nitroalkynes 6, which were subsequently reduced in the presence of tin(II) chloride ( $SnCl_2$ ) to provide the corresponding aminoalkynes 7 (Scheme 1). Sulfonylation of the anilines were conducted in the presence of the desired sulfonyl chloride using pyridine as solvent. Indoles 9 were obtained by cyclization of the alkyne precursors 8 in the presence of copper acetate ( $Cu(OAc)_2$ ),<sup>25</sup> at reflux of dichloroethane ( $C_2H_4Cl_2$ ), or under microwave irradiations at 130–150 °C. Deprotection of the esters with lithium hydroxide (LiOH), in a mixture of tetrahydrofuran (THF) and water, yielded the desired carboxylic acid compounds 4 and 10.

When the nitro starting material was not available, the synthesis was started from the corresponding commercially available iodoaniline bearing the desired substitutions (Scheme 2). The sulfonylation reaction was carried out with various aryl sulfonyl chlorides in pyridine. Most of the time, over reaction was observed yielding a mixture of disulfonylated and mono-sulfonylated compounds. Conveniently direct treatment of the crude mixture with a 3 M potassium hydroxide (KOH) solution allowed to convert the undesired bis-capped product back to the wanted iodosulfonamide 11. Sonogashira cross coupling in the presence of bis(triphenylphosphine)palladium(II) dichloride ( $Pd(PPh_3)_2Cl_2$ ), copper iodide (CuI), and diethylamine ( $Et_2N$ ) in dimethylformamide (DMF) under microwave heating led directly to the indoles 12. Final saponification provided derivatives 13 and 5.

The synthesis sequence depicted in Scheme 3 started with a Sonogashira reaction between substituted commercially available iodoanilines and *tert*-butyl hex-5-ynoate. Compounds 14 were treated with  $Cu(OAc)_2$ ,<sup>22</sup> under microwave conditions at 130 °C for 40 min, to provide indoles 15. Deprotonation with sodium hydride (NaH) followed by addition of arylsulfonyl chlorides gave the corresponding sulfonyl indoles, which were



**Figure 2.** From HTS hit to clinical candidate.

Scheme 1. Synthesis of Indole Derivatives via Nitroalkyne Intermediates<sup>a</sup>

<sup>a</sup>Reagents and conditions: (a) alkyne, Pd(PPh<sub>3</sub>)<sub>4</sub>, CuI, TEA, DMF; (b) SnCl<sub>2</sub>, AcOEt, EtOH; (c) ArSO<sub>2</sub>Cl, pyridine; (d) Cu(OAc)<sub>2</sub>, 1,2-dichloroethane reflux or microwave (130–150 °C); (e) LiOH·H<sub>2</sub>O, THF/H<sub>2</sub>O.

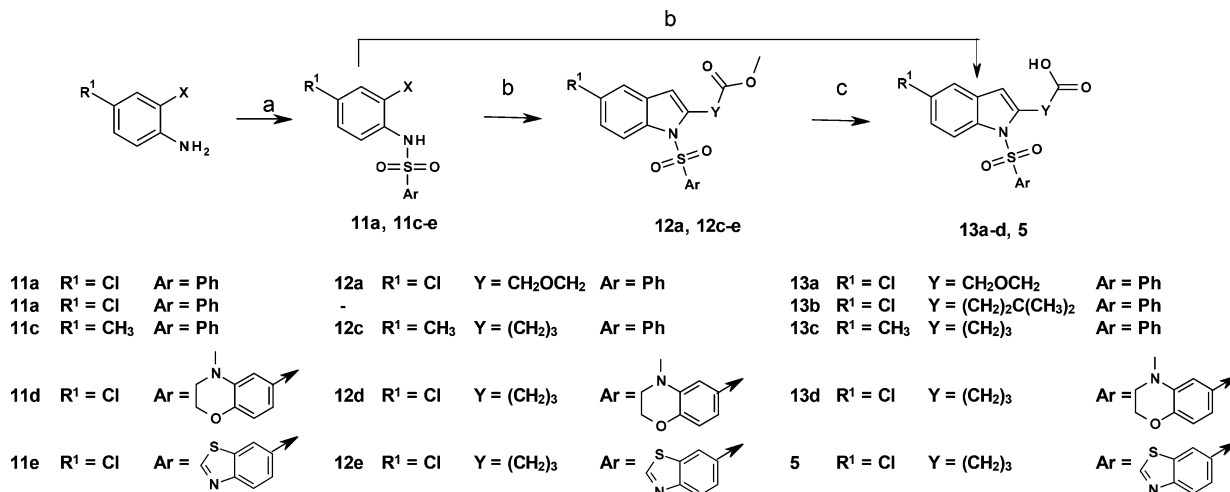
subsequently deprotected with trifluoroacetic acid (TFA) to readily afford derivatives 16.

Compound 22 was prepared according to the synthetic pathway depicted in Scheme 4. Sulfonation of 7b with 4-fluoro-3-nitro-benzenesulfonyl chloride in a mixture of pyridine and 2-(dimethylamino)pyridine (DMAP) lead to 17, which was cyclized in the presence of Cu(OAc)<sub>2</sub> to the indole 18. Nucleophilic substitution of the fluorine atom by aqueous ammonia led to 19. The benzimidazole moiety 21 was obtained by reduction of the nitro group with iron powder in acetic acid followed by cyclization in the presence of formic acid. Finally, hydrolysis with LiOH in a THF–water mixture afforded compound 22.

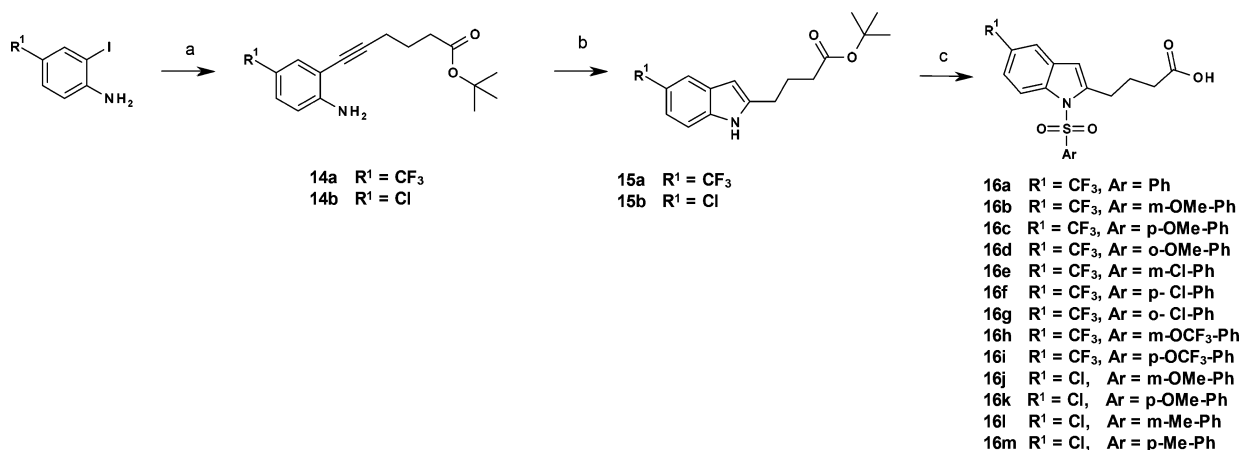
**In Vitro Structure–Activity Relationship (SAR).** Compounds were evaluated for human PPAR in vitro potency and

efficacy using a cell based Gal-4 transactivation assays in CV-1 simian in origin with SV40 gene (COS-7) cells transfected with hPPAR $\alpha$ , hPPAR $\delta$ , or hPPAR $\gamma$  ligand binding domains (LBD).  $E_{\max}$  was measured relatively to fenofibric acid<sup>26</sup> for PPAR $\alpha$ , 1a for PPAR $\gamma$ , and GW501516<sup>27</sup> for PPAR $\delta$ .

**Investigating the Chain Linker.** To establish basic SAR information, we started the optimization with analogs bearing different types of linker between the indole moiety and the acidic headgroup (Table 1). Modification of the linker led to noticeable changes in the PPAR subtype activity. As already mentioned, the two carbon atom unit linker, compound 4, imparted potent PPAR $\alpha$  transactivation activity, but weak PPAR $\delta$  and  $\gamma$  ones. Extending to a three carbon atom chain, 10b, led to a decreased PPAR $\alpha$  activity and increased both PPAR  $\delta$  and  $\gamma$  ones. The lengthening to a four carbon atom unit chain, 10c, or

Scheme 2. Synthesis of Indole Derivatives via Halogenosulfonamide Intermediates<sup>a</sup>

<sup>a</sup>Reagents and conditions: (a) (i) ArSO<sub>2</sub>Cl, pyridine; (ii) KOH, dioxane, reflux; (b) alkyne, Pd(PPh<sub>3</sub>)<sub>2</sub>Cl<sub>2</sub>, CuI, diethylamine, DMF, microwave 130 °C; (c) LiOH·H<sub>2</sub>O, THF/H<sub>2</sub>O.

Scheme 3. Synthesis of Indole Derivatives via Indole NH Intermediates<sup>a</sup>

<sup>a</sup>Reagents and conditions: (a) *tert*-butyl hex-5-ynoate, Pd(PPh<sub>3</sub>)<sub>2</sub>Cl<sub>2</sub>, CuI, diethylamine, DMF, microwave 130 °C; (b) Cu(OAc)<sub>2</sub>, 1,2-dichloroethane, reflux or microwave (150 °C); (c) (i) NaH, ArSO<sub>2</sub>Cl, DMF; (ii) TFA, CH<sub>2</sub>Cl<sub>2</sub>.

the introduction of a heteroatom in the chain, **13a**, led to a total loss of activity. As could be expected from previously described PPAR $\alpha$  selective compounds, the addition of a substituent at the  $\alpha$  position of the carbonyl group, indeed, resulted in a selective PPAR $\alpha$  agonist **13b**. Finally, compound **10b** with a three carbon atom chain demonstrated the best balanced pan PPAR profile in terms of potency, with partial efficacy ( $E_{\max}$  in the range of 50%).

**Investigating the Substitution of the Indole.** To further explore the activity and pan PPAR profile of this series, the investigation focused on the substitution of the indole ring (Table 2). First, the 5-position was investigated. Only hydrophobic substituents, such as 5-chloro **10b**, 5-trifluoromethyl **16a**, and 5-methyl **13c** led to active compounds. The trifluoromethyl (CF<sub>3</sub>) substitution **16a** yielded a dual PPAR $\alpha/\gamma$  agonist compound, very close in terms of potency and efficacy to the parent compound **4** but still with a less balanced pan PPAR profile compared to compound **10b**, which remained the best profile at this stage. On the contrary, the 5-methoxy **10d** was totally inactive.

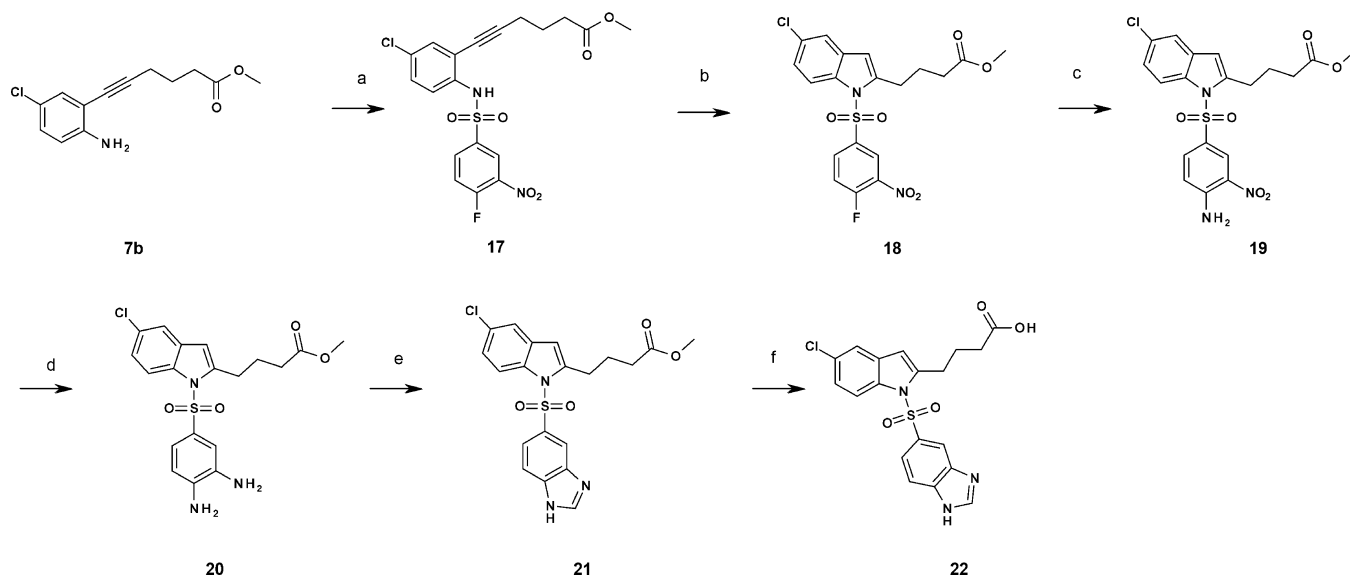
Additionally, a series of more hindered alkoxy chains (data not shown) were prepared, but unfortunately, these modifications were completely detrimental for pan PPAR activity.

The other positions of the indole scaffold were also investigated (data not shown). The 6-position turned out to be unfavorable for PPAR activity, while the 4-position led to a completely misbalanced profile.

**Investigating the Nature of the Aryl Sulfonamide.** Our efforts were first focused on the phenyl sulfonamide substitutions (Table 3). Substitutions in the *ortho* position (**16d**, **16g**) tend mostly to drastically reduce the agonistic activity against all three subtypes. The *meta* and *para* positions of the phenyl were explored using electron-donating and electron-withdrawing groups and led to active compounds leaning toward PPAR $\gamma$  activity. Furthermore, no difference was observed between electron-donating **16b** and electron-withdrawing **16e** groups in the *meta* position. The same tendency is observed for *para* substituted compounds **16c**, **16f**, and **16i**.

It was therefore concluded that *meta* and *para* substituted compounds were quite similar in terms of profile, and no electronic effect could be observed on this part of the molecule.

As described in Table 1, the three carbon atom spacer chain led to moderately potent compounds presenting, however, the desired balanced pan PPAR agonist activity. Similar profiles are obtained when the C5 indole position is substituted by CF<sub>3</sub> or chloro.

Scheme 4. Synthesis of Compound 22<sup>a</sup>

<sup>a</sup>Reagents and conditions: (a) 4-fluoro-3-nitro-benzenesulfonyl chloride, pyridine, DMAP, CH<sub>2</sub>Cl<sub>2</sub>; (b) Cu(OAc)<sub>2</sub>, 1,2-dichloroethane microwave (150 °C); (c) NH<sub>4</sub>OH, dioxane; (d) Fe, AcOH 60 °C; (e) HCOOH, 100 °C; (f) LiOH·H<sub>2</sub>O, THF/H<sub>2</sub>O.

Table 1. Transactivation Activity: Analogues of Compound 4 with Modification of the Y Linker<sup>a</sup>

compd	Y	hPPAR $\alpha$		hPPAR $\delta$		hPPAR $\gamma$	
		EC <sub>50</sub> (nM)	E <sub>max</sub> (%)	EC <sub>50</sub> (nM)	E <sub>max</sub> (%)	EC <sub>50</sub> (nM)	E <sub>max</sub> (%)
4	(CH <sub>2</sub> ) <sub>2</sub>	260 ± 34	101 ± 14	1912 ± 75	56 ± 18	1558 ± 1	43 ± 3
10b	(CH <sub>2</sub> ) <sub>3</sub>	956 ± 290	51 ± 19	645 ± 21	46 ± 10	284 ± 97	46 ± 10
10c	(CH <sub>2</sub> ) <sub>4</sub>	nd	<20	nd	<20	nd	<20
13a	CH <sub>2</sub> OCH <sub>2</sub>	nd	<20	nd	<20	nd	<20
13b	(CH <sub>2</sub> ) <sub>2</sub> C(CH <sub>3</sub> ) <sub>2</sub>	160 ± 24	90 ± 39	nd	<20	910 ± 135	32 ± 13

<sup>a</sup>E<sub>max</sub> = maximum activation in percent of control. compd = compound. nd = not determined. All EC<sub>50</sub> were mean of at least two independent experiments performed in triplicate.

Table 2. Transactivation Activity: Analogues of Compound 4 with Modification of the R<sup>1</sup> Substituent<sup>a</sup>

compd	R <sup>1</sup>	hPPAR $\alpha$		hPPAR $\delta$		hPPAR $\gamma$	
		EC <sub>50</sub> (nM)	E <sub>max</sub> (%)	EC <sub>50</sub> (nM)	E <sub>max</sub> (%)	EC <sub>50</sub> (nM)	E <sub>max</sub> (%)
10b	Cl	956 ± 290	51 ± 19	645 ± 21	46 ± 10	284 ± 97	46 ± 10
16a	CF <sub>3</sub>	1198 ± 406	48 ± 12	>5000	49 ± 15	417 ± 195	50 ± 9
13c	CH <sub>3</sub>	1300 ± 28	46 ± 29	>5000	45 ± 20	284 ± 80	38 ± 22
10d	OCH <sub>3</sub>	nd	<20	nd	<20	nd	<20

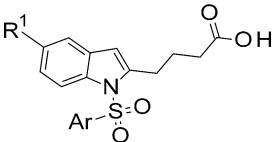
<sup>a</sup>E<sub>max</sub> = maximum activation in percent of control. compd = compound. nd = not determined. All EC<sub>50</sub> were mean of at least two independent experiments performed in triplicate.

Finally, it clearly appears that *meta* and *para* substitutions were the best options toward the wanted balanced profile.

The role of the phenyl group (south part of the molecule) was further investigated by exploring fused ring systems (Table 4). As expected, a fused ring mimicking the *ortho* substitution led

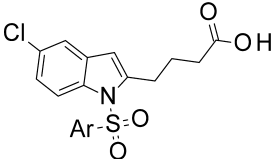
to a drastic decrease in PPAR activity. For example, 1-naphthyl sulfonamide derivative 10g showed a significantly reduced efficacy on PPAR $\gamma$  and no activity at all on PPAR $\delta$ . Efforts were then focused on other fused rings mimicking *meta* or *para* substitutions that were shown to be more in line with our

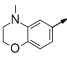
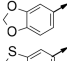
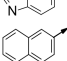
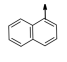
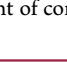


Table 3. Transactivation Activity: Analogues of Compound 4 with Modification of the R<sup>1</sup> and Ar Substituents<sup>a</sup>


compd	R <sup>1</sup>	Ar	hPPAR $\alpha$		hPPAR $\delta$		hPPAR $\gamma$	
			EC <sub>50</sub> (nM)	E <sub>max</sub> (%)	EC <sub>50</sub> (nM)	E <sub>max</sub> (%)	EC <sub>50</sub> (nM)	E <sub>max</sub> (%)
10b	Cl	Ph	956 ± 290	51 ± 19	645 ± 21	46 ± 10	284 ± 97	46 ± 10
16b	CF <sub>3</sub>	<i>m</i> -OMe-Ph	1164 ± 352	37 ± 23	1607 ± 453	28 ± 12	65 ± 34	46 ± 14
16c	CF <sub>3</sub>	<i>p</i> -OMe-Ph	764 ± 218	55 ± 2	1259 ± 393	24 ± 4	82 ± 19	38 ± 8
16d	CF <sub>3</sub>	<i>o</i> -OMe-Ph	>5000	35 ± 23	nd	<20	1248 ± 447	35 ± 14
16e	CF <sub>3</sub>	<i>m</i> -Cl-Ph	2421 ± 229	70 ± 5	2026 ± 149	21 ± 3	256 ± 171	49 ± 12
16f	CF <sub>3</sub>	<i>p</i> -Cl-Ph	2824 ± 326	45 ± 27	1650 ± 636	38 ± 13	629 ± 359	36 ± 13
16g	CF <sub>3</sub>	<i>o</i> -Cl-Ph	>5000	104 ± 8	nd	<20	>5000	45 ± 1
16h	CF <sub>3</sub>	<i>m</i> -OCF <sub>3</sub> -Ph	2756 ± 287	50 ± 19	1140 ± 26	23 ± 11	201 ± 141	39 ± 6
16i	CF <sub>3</sub>	<i>p</i> -OCF <sub>3</sub> -Ph	1963 ± 1425	40 ± 18	2100 ± 1273	28 ± 11	573 ± 292	32 ± 14
16j	Cl	<i>m</i> -OMe-Ph	305 ± 35	40 ± 19	1230 ± 449	43 ± 7	55 ± 18	48 ± 10
16k	Cl	<i>p</i> -OMe-Ph	419 ± 122	26 ± 10	nd	<20	72 ± 59	25 ± 4
16l	Cl	<i>m</i> -Me-Ph	1250 ± 281	59 ± 22	1347 ± 251	42 ± 6	75 ± 25	46 ± 10
16m	Cl	<i>p</i> -Me-Ph	>5000	36 ± 10	1085 ± 78	29 ± 3	277 ± 117	30 ± 9

<sup>a</sup>E<sub>max</sub> = maximum activation in percent of control. compd = compound. nd = not determined. All EC<sub>50</sub> were mean of at least two independent experiments performed in triplicate.

Table 4. Transactivation Activity: Analogues of Compound 4 with Modifications of the Ar Substituent,<sup>a</sup> Part 1


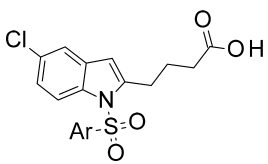
compd	Ar	hPPAR $\alpha$		hPPAR $\delta$		hPPAR $\gamma$	
		EC <sub>50</sub> (nM)	E <sub>max</sub> (%)	EC <sub>50</sub> (nM)	E <sub>max</sub> (%)	EC <sub>50</sub> (nM)	E <sub>max</sub> (%)
10b	Ph	956 ± 290	51 ± 19	645 ± 21	46 ± 10	284 ± 97	46 ± 10
13d		410 ± 107	113 ± 44	697 ± 271	54 ± 6	16 ± 3	48 ± 10
10e		790 ± 339	77 ± 21	977 ± 134	43 ± 9	71 ± 12	45 ± 11
5		1537 ± 278	106 ± 30	866 ± 180	105 ± 16	206 ± 71	79 ± 15
10f		nd	<20	nd	<20	35 ± 3	34 ± 7
10g		901 ± 435	67 ± 16	nd	<20	265 ± 131	36 ± 8

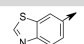
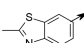
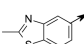
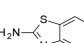
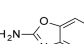
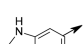
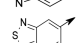
<sup>a</sup>E<sub>max</sub> = maximum activation in percent of control. compd = compound. nd = not determined. All experiments were performed in triplicate in at least two independent experiments.

objectives to reach a pan PPAR balanced profile. Surprisingly 2-naphthyl **10f** showed very low potency on all three PPARs. It was observed, at this stage, that nonconjugated fused rings like benzo[1,3]dioxole **10e** and *N*-methyl benzomorpholine **13d** led to very active compounds but with misbalanced potency in favor of the PPAR $\gamma$ . The conjugated fused ring benzothiazole analogue **5** displayed high efficacy on all PPARs subtypes and the best balanced profile in terms of potency.

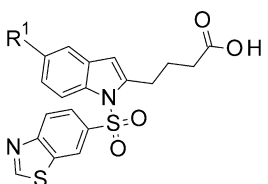
At this stage, it was decided to investigate more in depth the potential of the benzothiazole moiety, by introducing a series of different heteroaromatic rings (Table 5). Unfortunately, the 5-sulfonylbenzothiazole, isomer 4-[1-(1,3-benzothiazol-5-ylsulfonyl)-5-chloro-indol-2-yl]butanoic acid, of compound **5** was

not prepared due to chemical stability issues of the corresponding sulfonyl chloride intermediate. In order to investigate the influence of substitution at position 2 of the benzothiazole, we decided to prepare the methylated derivatives of both benzothiazole isomers, compound **10i** (1,3-benzothiazol-5-ylsulfonyl) and compound **10h**, 1,3-benzothiazol-6-ylsulfonyl. These derivatives ended to be much less efficient than **5** on both PPAR $\alpha$  (E<sub>max</sub>(**10h**) < 20%, E<sub>max</sub>(**10i**) = 22%, E<sub>max</sub>(**5**) = 106%) and PPAR $\delta$  (E<sub>max</sub>(**10h**) = 27%, E<sub>max</sub>(**10i**) = 20%, E<sub>max</sub>(**5**) = 105%) while keeping some efficacy against PPAR $\gamma$  (E<sub>max</sub>(**10h**) = 36%, E<sub>max</sub>(**10i**) = 39%, E<sub>max</sub>(**5**) = 79%). At last, it became clear that there was no advantage to use the other isomer of the benzothiazole, as the final picture of PPAR activity was

Table 5. Transactivation Activity: Analogues of Compound 4 with Modification of the Ar Substituent,<sup>a</sup> Part 2


compd	Ar	hPPAR $\alpha$		hPPAR $\delta$		hPPAR $\gamma$	
		EC <sub>50</sub> (nM)	E <sub>max</sub> (%)	EC <sub>50</sub> (nM)	E <sub>max</sub> (%)	EC <sub>50</sub> (nM)	E <sub>max</sub> (%)
5		1537 ± 278	106 ± 30	866 ± 180	105 ± 16	206 ± 71	79 ± 15
10h		nd	<20	441 ± 292	27 ± 7	11 ± 1	36 ± 6
10i		2360 ± 127	22 ± 3	1098 ± 114	20 ± 7	175 ± 88	39 ± 8
10j		1263 ± 25	57 ± 6	919 ± 79	82 ± 11	41 ± 8	74 ± 3
10k		>5000	44 ± 20	1387 ± 317	66 ± 16	378 ± 111	52 ± 19
22		>5000	43	>5000	20	>5000	42
10l		>5000	81	>5000	35	153	67

<sup>a</sup>E<sub>max</sub> = maximum activation in percent of control. compd = compound. nd = not determined. All EC<sub>50</sub> were mean of at least two independent experiments performed in triplicate. Values based on single experiment run in triplicate are indicated in italics.

Table 6. Transactivation Activity: Exploring the R<sup>1</sup> Substituent of Compound 5<sup>a</sup>


compd	R <sup>1</sup>	hPPAR $\alpha$		hPPAR $\delta$		hPPAR $\gamma$	
		EC <sub>50</sub> (nM)	E <sub>max</sub> (%)	EC <sub>50</sub> (nM)	E <sub>max</sub> (%)	EC <sub>50</sub> (nM)	E <sub>max</sub> (%)
5	Cl	1537 ± 278	106 ± 30	866 ± 180	105 ± 16	206 ± 71	79 ± 15
10m	CF <sub>3</sub>	1620 ± 430	82 ± 14	1120 ± 161	79 ± 13	147 ± 12	70 ± 7

<sup>a</sup>E<sub>max</sub> = maximum activation in percent of control. compd = compound. All EC<sub>50</sub> were mean of at least two independent experiments performed in triplicate.

completely unbalanced. Replacing the methyl group on the position 2 of the benzothiazole with an amino group compound **10j** allowed to regain activity on PPAR $\alpha$  and PPAR $\delta$  but also increased the unbalance toward PPAR $\gamma$  with EC<sub>50</sub> of 41 nM. Moving to the corresponding benzoxazole **10k** allowed to obtain a compound well balanced for PPAR $\delta$  and PPAR $\gamma$  but less potent on PPAR $\alpha$ . To conclude on this part, all the tested substitutions on the 2-position (**10h**, **10i**, **10j**, and **10k**) led to an unbalanced profile, and the naked compound **5** remained the best regarding the wanted profile.

Alternative 5,6-heteroaromatic rings containing compounds, like the benzimidazole **22** and benzothiadiazole **10l**, display low potency or unbalanced profile.

Finally, all the produced derivatives demonstrated lower efficacy, potency, or unbalanced profile in comparison to compound **5**. These findings prompted us to retain the benzothiazole substituent on the south part of the molecule as the most preferred option for the desired pan PPAR profile.

Reverting to the core ring investigation, the 5-CF<sub>3</sub> substitution on the indole, which was favorable on the earlier phenyl series (**16a**, Table 2), surprisingly turned out to be similar in

terms of potency but less efficient in this more evolved benzothiazole series (**10m**, Table 6), and only the 5-chloro analog **5** retained the desired balanced pan PPAR profile.

**Physicochemical Properties and Pharmacokinetic Profiling.** The promising in vitro human results obtained with this novel indolsulfonamides series have motivated further investigation to demonstrate their potential to become preclinical development compounds.

The drug-like properties of the most promising compound **5** were examined to determine its suitability for further investigation.

Aqueous solubility and permeability are two major players that determine oral bioavailability. Despite its low solubility, compound **5**, as well as the original hit **4**, showed a very strong permeability profile compared to Warfarin (Table 7).

**Functional Activity: Beta-Oxidation in Human Hepatocytes and Mouse Myoblast Cell Line.** Functional PPAR activity for all three subtypes was determined in a panel of in vitro assays. Fatty acid beta-oxidation was used as a marker of PPAR $\alpha$  and PPAR $\delta$  activation. They were respectively evaluated in human hepatoma cell line (HuH7) and in mouse myoblast cell line (C2C12). The PPAR $\gamma$  functional

Table 7. In Vitro Permeability of Selected Analogs

compd	Caco-2 mean Papp ( $\times 10^{-6}$ cm/s) neat/FASSIF			solubility ( $\mu$ M)
	A $\rightarrow$ B	B $\rightarrow$ A	efflux ratio	
5	24	0.2	0.1	8.7
4	61	14.4	0.2	9
Warfarin	39.8	0.7	0.02	56

activity was measured in human adipocytes through the expression of adiponectin and adipocyte protein 2 (aP2) genes, using **1a** at 1  $\mu$ M as reference.

As can be observed in Table 8, compound **5** demonstrated significant activation of PPAR $\alpha$  and PPAR $\delta$  as indicated by increasing levels of beta-oxidation on HuH7 and C2C12 consistent with the observed transactivation data. Compound **5** induced 45% beta-oxidation at 1  $\mu$ M in HuH7 and a significant effect in C2C12 at 3  $\mu$ M, while compound **4** showed beta-oxidation activation on HuH7 only at 10  $\mu$ M and no effect on C2C12. The best dose response profile on beta-oxidation in both human hepatocytes and mouse myoblasts was observed with compound **5** in comparison to compound **4**. Similar conclusion can be drawn from the induction of PPAR $\gamma$  target genes adiponectin and aP2 expression (Table 9). A clear dose response effect is observed, despite a slight decrease at the highest concentration, i.e., 30  $\mu$ M, which could be attributed to partial compound precipitation.

**In Vivo Pharmacokinetic Studies.** Encouraged by the promising in vitro results, the pharmacokinetic parameters of the best candidate, compound **5**, were determined in common a strain of laboratory mouse (C57Bl6) (Table 10). Eight animals were dosed orally with **5** (10 mg/kg), and plasma samples were collected over a 24 h period. The preliminary data suggested a once daily dose.

Interestingly, compound **5** was detected in plasma in the microgram range (maximum serum concentration that a drug achieves in a specific compartment ( $C_{\max}$ ) = 10.7  $\mu$ g/mL), well above the  $EC_{50}$  value, which aligns well with the measured solubility, human Caucasian colon adenocarcinoma (Caco-2) permeability, and absorption data. This overall satisfactory profile provided solid evidence that this new generation of pan PPAR derivatives were well suited for evaluation in animal disease models.

**In Vivo Pharmacological Studies. db/db Mouse Model.** Before moving to the in vivo models, it was established that compound **5** exhibited similar potency and efficacy for human and mouse PPARs as measured in chimeric galactose-responsive

Table 10. Compound 5 Plasma Pharmacokinetic Parameters Following Single Oral Dose (10 mg/kg in Methyl Cellulose as Vehicle) in C57Bl6 Mice

compd	$C_{\max}$ (ng/mL) <sup>a</sup>	$T_{\max}$ (h) <sup>a</sup>	AUCinf <sup>a</sup> (h·(ng/mL))
5	10710	1	29367
4	14590	1	37286
10b	11850	1	51082

<sup>a</sup>Single measurement.

transcription factor (Gal-4) human or mouse PPAR-mediated reporter gene assays (Table 11).

The antidiabetic effect of compound **5** was evaluated in *db/db* mice, an obese rodent model<sup>28</sup> of type 2 diabetes characterized by severe insulin resistance, hypertriglyceridemia and marked hyperglycemia.

Compounds were administered orally once daily for 5 days for **5** and 10 days for **4**, to homozygous C57BL/Ks-db male mice (*db/db* mice). A blood sample was taken from the retro-orbital sinus before treatment and 4 h after the last gavage. Triglycerides and glucose levels were measured after plasma collection. The results are expressed in % variation on the final day relative to the control group (Figure 3).

As would be expected from a pan PPAR agonist, treatment of *db/db* mouse with compound **5** induced a dose-dependent and significant decrease of circulating glucose levels: 40% at 10 mg/kg and 58% at 30 mg/kg. In the same study, abnormal plasma triglyceride levels observed in this disease model were markedly corrected following treatment with compound **5**: 33% at 10 mg/kg and 45% at 30 mg/kg (Figure 3). On the contrary, compound **4**, the initial hit, had nonsignificant effect on triglycerides levels and moderate decrease of circulating glucose at 10 mg/kg, which was improved at 30 mg/kg.

**Carbon Tetrachloride (CCl<sub>4</sub>)-Induced Liver Fibrosis in Mice.**<sup>29</sup> Liver fibrosis is a critical hallmark of NASH, being associated with long-term overall mortality in patients. Fibrosis is characterized by an excessive synthesis of extra-cellular matrix composed of collagen and fibronectin. CCl<sub>4</sub> induced liver fibrosis is a well-documented model to investigate potential antifibrotic properties of pharmacological agents, the evaluation of antifibrotic activity being determined by the measurement of collagen deposition in the liver.

Collagen deposition measured by picrosirius red (PSR) staining on liver histological sections was significantly higher in CCl<sub>4</sub>-vehicle treated mice than in saline injected mice. Treatment with compound **5** at 10 and 30 mg/kg, orally once a day, produced a dose-dependent and significant reduction of

Table 8. Cellular Activities: Beta-Oxidation in HuH7 and C2C12 at Different Concentrations<sup>a</sup>

compd	HuH7 (% beta-oxidation)				C2C12 (% beta-oxidation)			
	1 $\mu$ M	3 $\mu$ M	10 $\mu$ M	30 $\mu$ M	1 $\mu$ M	3 $\mu$ M	10 $\mu$ M	30 $\mu$ M
5	44 $\pm$ 10	79	113 $\pm$ 23	120 $\pm$ 9	12 $\pm$ 9	37	67 $\pm$ 9	55 $\pm$ 8
4	5 $\pm$ 12		45 $\pm$ 2	96 $\pm$ 19	−6 $\pm$ 4		12 $\pm$ 12	27 $\pm$ 7

<sup>a</sup>All values are mean of at least two independent experiments run in triplicate. Values based on single experiment run in triplicate are indicated in italics. compd = compound.

Table 9. Cellular Activities: Gene Expression of aP2 and Adiponectin in Adipocytes at Different Concentrations of **5**<sup>a</sup>

compd 5	0.1 $\mu$ M	0.3 $\mu$ M	1 $\mu$ M	3 $\mu$ M	10 $\mu$ M	30 $\mu$ M
aP2	6 $\pm$ 1	18 $\pm$ 4	47 $\pm$ 1	78 $\pm$ 18	97 $\pm$ 3	70 $\pm$ 12
adiponectin	7 $\pm$ 1	16 $\pm$ 1	42 $\pm$ 8	62 $\pm$ 6	80 $\pm$ 6	56 $\pm$ 3

<sup>a</sup>Percent expression vs **1a** @ 1  $\mu$ M accounting for 100%. All values are means of three independent experiments run in triplicate. compd = compound.



Table 11. Agonistic Effect of Compound 5 on Human and Mouse PPARs Isoforms<sup>a</sup>

	PPAR $\alpha$		PPAR $\delta$		PPAR $\gamma$	
	EC <sub>50</sub> (nM)	E <sub>max</sub> (%)	EC <sub>50</sub> (nM)	E <sub>max</sub> (%)	EC <sub>50</sub> (nM)	E <sub>max</sub> (%)
human	1537 $\pm$ 278	106 $\pm$ 30	866 $\pm$ 180	105 $\pm$ 16	206 $\pm$ 71	79 $\pm$ 15
mouse	366 $\pm$ 71	72 $\pm$ 14	1560 $\pm$ 279	131 $\pm$ 30	202 $\pm$ 48	73 $\pm$ 17

<sup>a</sup>E<sub>max</sub> = maximum activation in percent of control. All experiments were performed in triplicate in at least three independent experiments.

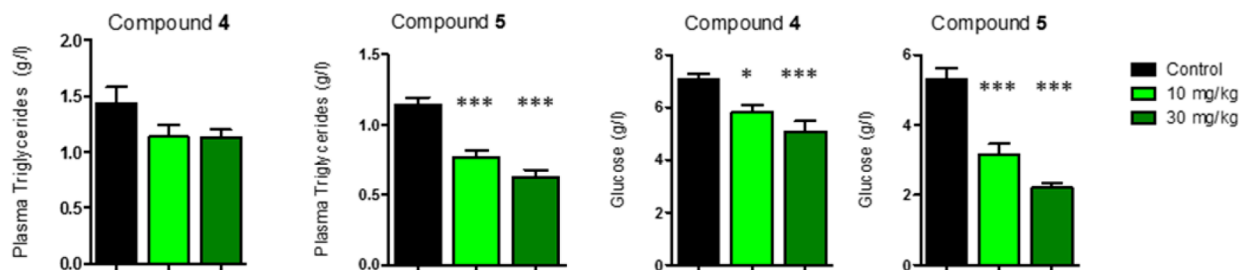


Figure 3. Compounds 4 and 5: Percentage reduction of plasma glucose and triglycerides in *db/db* mice. Mice were dosed qd with 10 or 30 mg/kg for 5 days with 5 and 10 days with 4. \**P* < 0.05, \*\*\**P* < 0.001 versus control (one-way analysis of variance followed by Dunnett's test).

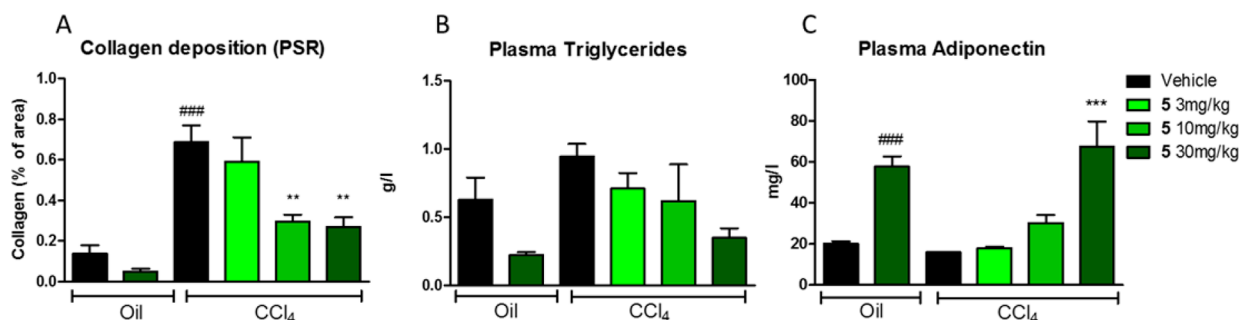


Figure 4. Effects of compound 5 at 3, 10, and 30 mg/kg on collagen deposition, plasma triglycerides, and adiponectin in CCl<sub>4</sub>-induced liver fibrosis in mice after 3 weeks of treatment. \*\**P* < 0.01, \*\*\**P* < 0.001 versus vehicle CCl<sub>4</sub>; ###*P* < 0.001 versus vehicle oil (one-way analysis of variance followed by Dunnett's test).

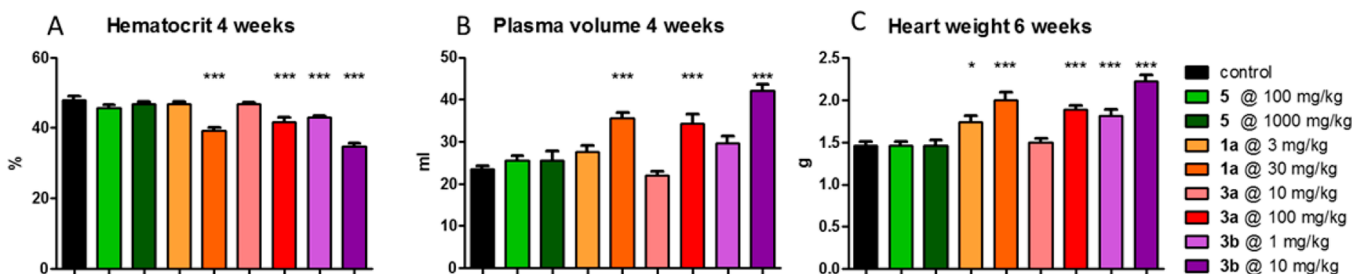


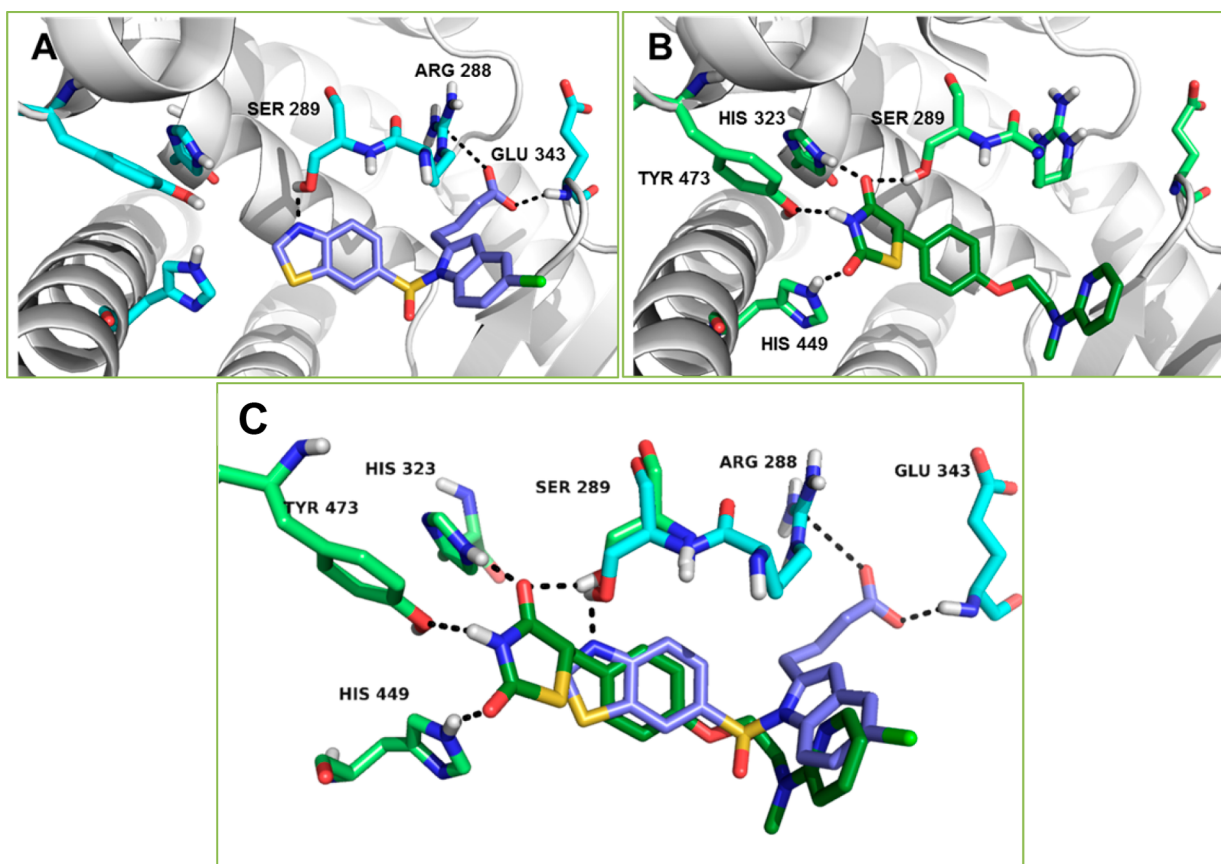
Figure 5. Effects of compound 5 at 100 and 1000 mg/kg on hematocrit, plasma volume, and heart weight after 4 and 6 weeks of treatment in Sprague–Dawley rats, comparison with the PPAR $\gamma$  and dual PPAR $\alpha/\gamma$  agonists 3a, 3b, and 1a. \**P* < 0.05, \*\*\**P* < 0.001 versus control (one-way analysis of variance followed by Dunnett's test).

collagen deposition. In parallel, and consistently with panPPAR activation, compound 5 produced a significant reduction in plasma triglycerides levels, a marker of PPAR $\alpha/\delta$  engagement, and a significant elevation of plasma adiponectin levels, a marker of PPAR $\gamma$  engagement (Figure 4).

**Hemodilution, Plasma Volume Expansion, and Heart Weight Increase in Rats.** Contrasting with first generation PPAR $\gamma$  agonists like 3a, 3b, or 1a, compound 5 had no effect on hematocrit, plasma volume or heart weight. All the three other PPAR $\gamma$  agonists mentioned above that were evaluated in this study induced a significant reduction in hematocrit levels and a significant increase in plasma volume after 4 weeks of treatment at the highest dose. These compounds, but not compound 5,

showed marked increase in heart weight after 6 weeks of treatment (Figure 5).

**Xray PPAR $\gamma$  Structure with Compound 5 in Comparison to 1a.** Numerous PPAR $\gamma$  structures have been described in the protein database (PDB). PPAR's ligand binding domain classically consists of 12  $\alpha$ -helices and 4 beta-stranded sheets. PPAR $\gamma$ 's ligand binding pocket (LBP) is large (1300 Å<sup>3</sup>) with Y- or T-shape. Different binding modes of ligands are observed in PPAR $\gamma$ 's LBP. Ligands may bind in different locations in the LBP (3K8S,<sup>30</sup> 3GBK,<sup>31</sup> and 4PWL<sup>32</sup>), and on some occasions, two ligands can be accommodated at the same time (4BCR<sup>33</sup>). Compound 1a (dark green) (Figure 6B) is a potent PPAR $\gamma$  agonist. It binds in a U-shape conformation, wrapping itself



**Figure 6.** (A) Cocrystal structure of compound **5** (purple) with PPAR $\gamma$  LBD (6ENQ). (B) Cocrystal structure of compound **1a** (dark green) with PPAR $\gamma$  LBD (1FM6). (C) Superposition of compound **5** (purple) and **1a** (dark green) in PPAR $\gamma$  LBD.

around Helix3 (1FM6<sup>34</sup>). The thiazolidinedione headgroup, which mimics the usually encountered carboxylic acid moiety present in PPAR's natural ligands such as fatty acids (e.g., 2VV2<sup>35</sup>), interacts directly with Helix12 via multiple hydrogen bonds. The thiazolidinedione's nitrogen atom binds to Y473 and its two carbonyl groups to H323 and H449. Differently from **1a** (dark green), compound **5** (purple) (Figure 6A) does not interact directly with Helix12 even if it stabilizes a conformationally active form of PPAR $\gamma$ . It adopts a T-shape conformation partially overlapping with the U-shape of **1a** (Figure 6C) and filling an additional subpocket with specific hydrogen bond interactions between its carboxylic acid and both E343 and R288.

**Cofactors Recruitment by Compound 5 vs 1a.** It is now known from genetic and pharmacological studies that moderately activating compound can lead to better therapeutic outcomes compared to full activation.<sup>36</sup> These observations have been translated into the concept of PPAR partial agonists and selective PPAR modulators (SPPARMs),<sup>37,38</sup> leading to differential cofactor recruitment profiles, and finally different gene expression patterns.<sup>39</sup> The cofactor recruitment profiles induced by compounds **5** and **1a** were evaluated in a time-resolved fluorescence energy transfer (TR-FRET) assay using a panel of coactivators and corepressors, for the determination and comparison of their respective potency and efficacy on PPAR $\gamma$ .

Comparatively to **1a**, compound **5** displayed significant differences in cofactor recruitment both in terms of potency (Figure 7B) and efficacy (Figure 7A). For example, the nuclear receptor corepressor 1 (NCoR-ID1) and silencing mediator of retinoic acid and thyroid hormone receptor (SMRT) were both

"derecruited" by compounds **5** and **1a**, but with a 10-fold lower potency for compound **5**. EC<sub>50</sub> respectively were 4097 nM vs 326 nM for NCoR-ID1 and 1140 nM vs 95 nM for SMRT (Table 12).

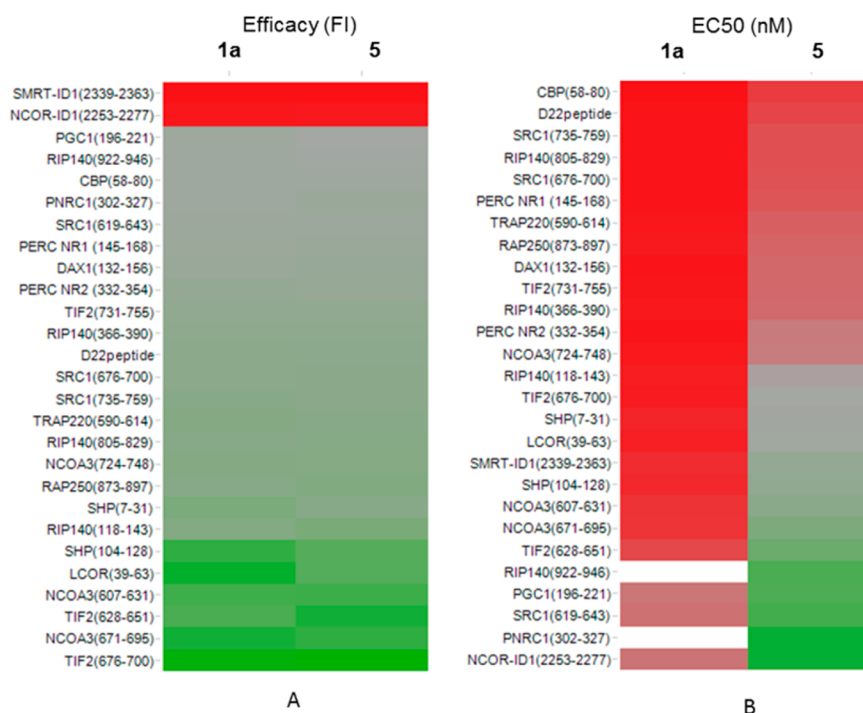
Major differences in potency were also noticed for nuclear receptor coactivator 3 (NCoA3), steroid receptor coactivator 1 (SRC-1), PPAR $\gamma$  coactivator-1 $\alpha$  (PGC1 $\alpha$ ), receptor interacting protein 140 (RIP140), and proline-rich nuclear receptor coactivator 1 (PNRC1) recruitment. When considering efficacy, compound **5** showed a partial agonist activity for PGC1 $\alpha$  and ligand-dependent corepressor (LCOR), and a greater efficacy for PNRC1 in comparison to **1a**.

Collectively with the transactivation data (Table 4), these results demonstrated that compound **5** could be considered as a moderately potent and partial agonist on PPAR $\gamma$ , leading to differential gene expression as shown on aP2 and adiponectin (Table 9).

Altogether, the moderate potency of compound **5**, its different coregulator recruitment profile, and its balanced activity for the three PPAR isoforms may well explain its good safety profile relatively to other PPAR $\gamma$  agonists.<sup>40,41</sup>

## CONCLUSION

In summary, we have described the synthesis and optimization of a new indole series. These compounds are characterized by their balanced activity on all PPAR subtypes. Compound **5** demonstrated excellent antihyperglycemic and hypolipidemic efficacy in the *db/db* mouse model and a significant antifibrotic activity in the mouse CCl<sub>4</sub>-induced liver fibrosis model. Contrasting with other PPAR $\gamma$  agonists, compound **5** had no



**Figure 7.** Dendograms of cofactor recruitment profiles for compounds 5 and 1a. (A) Efficacy, scale: red, FI < 1 derecruitment; gray, FI = 1 no activity; green, FI > 1 recruitment. (B) Potency, scale: red, 10 nM; gray, 500 nM; green, 5000 nM.

**Table 12.** Cofactors Recruitment Comparison Compound 5 vs 1a

peptide	1a			5		
	EC <sub>50</sub> (nM)	E <sub>min/max</sub> (FI)	E <sub>max</sub> (%)	EC <sub>50</sub> (nM)	E <sub>min/max</sub> (FI)	E <sub>max</sub> (%)
SMRT-ID1 (2339–2363)	95	0.06	100	1140	0.06	100
NCoR-ID1 (2253–2277)	326	0.1	100	4097	0.1	100
LCOR (39–63)	52	15.5	100	727	10.6	68
NCoA3 (607–631)	114	12.2	100	1484	12.4	102
NCoA3 (671–695)	117	14.2	100	1917	13.3	93
PGC1α (196–221)	332	2.3	100	3208	1.5	64
PNRC1 (302–327)	NC	1.9	100	4111	2.7	142
RIP140 (922–946)	NC	1.95	100	3274	1.7	88
SRC-1 (619–643)	316	2.3	100	3408	2.6	111

effect on hematocrit, plasma volume, or heart weight in rats. These encouraging results prompted us to further develop lanifibranor 5 for the treatment of NASH.

## EXPERIMENTAL SECTION

**Chemistry. General Methods.** Reagents and solvents obtained from commercial suppliers are used without further purification unless otherwise stated. All compounds are >95% pure by LC/MS analysis. All final compounds were characterized by <sup>1</sup>H NMR and <sup>13</sup>C NMR using a Bruker Avance 300, 400, or 500 MHz spectrometer. Chemical shifts are reported in ppm (δ) and were calibrated using the undeuterated solvent resonance as internal standard. Melting points were determined on a hot stage apparatus and are uncorrected. The liquid chromatography mass spectrum (LC/MS) analysis were carried out on a Waters ZQ mass spectrometer hyphenated to a chromatography system Agilent 1100 series including a photodiode array UV detector or on a Waters UPLC Acquity system including a photodiode array UV detector, an ELSD, and a mass spectrometer SCD. Method a: The gradient was 0–9 min, 5% B to 90% B; 9–11 min, 90% B; 11–12 min, 90% B to 10% B; 12–15 min, 10% B (0.6 mL/min flow rate). Mobile Phase A: 0.05% CF<sub>3</sub>COOH in water. Mobile Phase B: 0.05% CF<sub>3</sub>COOH in acetonitrile. Column: Uptispher OBD (Dimensions: 50 × 2 mm × 3 μm). Column temperature: 45 °C. UV detection: DAD

210–260 nm. MS detection (ESI positive and negative). Method b: The gradient was 0–0.1 min, 5% B; 0.1–2.3 min: 5% B to 95% B; 2.3–2.5 min, 95% B; 2.51–3 min, 5% B (0.8 mL/min flow rate). Mobile Phase A: 0.1% CH<sub>3</sub>COOH in water. Mobile Phase B: 0.1% CH<sub>3</sub>COOH in acetonitrile. Column: ACQUITY UPLC BEH C18 (Dimensions: 50 × 2.1 mm × 1.7 μm). Column temperature: 45 °C. UV detection: DAD 210–260 nm. MS detection (ESI positive and negative).

**3-[1-(Benzenesulfonyl)-5-chloro-indol-2-yl]propanoic Acid (4).** Compound 9a (180 mg, 0.46 mmol; 1 equiv) was mixed with 16 mL of THF and 4 mL of water, and 20 mg (0.48 mmol; 1.05 equiv) of lithium hydroxide (LiOH·H<sub>2</sub>O) was added. The mixture was stirred for 3 h at room temperature and then concentrated under reduced pressure. Water was added, and the solution was acidified with 1 N hydrochloric acid solution. The white precipitate was extracted with ethyl acetate, and the organic phase was dried over magnesium sulfate and concentrated under reduced pressure to give 160 mg of the expected product as a yellow solid (yield = 93%). mp = 165–168 °C. LC/MS (method a): R<sub>t</sub> = 5.35 min. MS m/z: 362 [M – H]<sup>–</sup>. <sup>1</sup>H NMR (400 MHz, DMSO-*d*<sub>6</sub>) δ 2.72 (t, J = 7.3 Hz, 2H), 3.24 (t, J = 6.8 Hz, 2H), 6.59 (s, 1H), 7.31 (dd, J = 8.8, 2.2 Hz, 1H), 7.59 (m, 3H), 7.70 (m, 1H), 7.83 (m, 2H), 8.02 (d, J = 9.0 Hz, 1H), 12.35 (br. s, 1H). <sup>13</sup>C NMR (126 MHz, DMSO-*d*<sub>6</sub>) δ 173.3, 142.4, 137.4, 134.8, 134.7, 130.8, 130.0, 128.3, 126.1, 124.0, 120.0, 115.6, 108.4, 32.4, 24.0.



4-[1-(1,3-Benzothiazol-6-ylsulfonyl)-5-chloro-indol-2-yl]butanoic Acid (**5**). This compound was prepared as described in the case of **4**, starting from **12e**, giving a 57% yield. White solid. mp = 182–185 °C. LC/MS (method a):  $R_t$  = 5.67 min. MS  $m/z$ : 433  $[M - H]^-$ .  $^1H$  NMR (500 MHz, DMSO- $d_6$ )  $\delta$  1.95 (m, 2H), 2.36 (t,  $J$  = 7.3 Hz, 2H), 3.09 (t,  $J$  = 7.5 Hz, 2H), 6.62 (s, 1H), 7.32 (dd,  $J$  = 8.9, 2.1 Hz, 1H), 7.57 (d,  $J$  = 2.1 Hz, 1H), 7.85 (dd,  $J$  = 8.6, 1.85 Hz, 1H), 8.10 (d,  $J$  = 8.9 Hz, 1H), 8.20 (d,  $J$  = 8.6 Hz, 1H), 8.98 (d,  $J$  = 1.9 Hz, 1H), 9.66 (s, 1H), 12.14 (br. s, 1H).  $^{13}C$  NMR (75 MHz, DMSO- $d_6$ ) shift 174.1, 162.5, 156.1, 143.0, 134.7, 134.6, 133.9, 130.9, 128.3, 124.2, 123.9, 123.4, 122.8, 119.9, 115.7, 108.7, 32.9, 27.7, 23.6.

**Methyl 5-(2-Amino-5-chloro-phenyl)pent-4-ynoate (7a).** 4-Chloro-2-iodo-nitrobenzene (35.5 g, 125 mmol; 1 equiv), 510 mL of triethylamine, 2.88 g (2.5 mmol; 0.02 equiv) of tetrakis-(triphenylphosphine)palladium, 0.72 g (3.75 mmol; 0.03 equiv) of cuprous iodide, and 50 mL of dimethylformamide were mixed. Fourteen grams (125 mmol; 1 equiv) of methyl pent-4-ynoate were then added at room temperature, and the reaction mixture was stirred for 24 h at room temperature. Toluene (100 mL) was added, and the solvents were evaporated. The residue was taken up with ethyl acetate and 1 N hydrochloric acid. The organic layer was washed with water, dried over magnesium sulfate, and concentrated under reduced pressure. Methyl 5-(5-chloro-2-nitro-phenyl)pent-4-ynoate **6a** was used crude in the next step. Stannous chloride (90.6 g, 400 mmol; 5 equiv), 70 mL of ethyl acetate, and 22 mL of ethanol were introduced into a round bottomed flask. This mixture was stirred for 15 min at room temperature, and a solution of 21.5 g (80 mmol; 1 equiv) of **6a** in 120 mL of ethyl acetate was then added slowly. The reaction mixture was stirred for 24 h at room temperature and then poured into a mixture of 200 g of ice and 200 mL of 1 N sodium hydroxide solution. The mixture was extracted twice with ethyl acetate; the combined organic phases were washed with water, dried over magnesium sulfate, and concentrated under reduced pressure. The oil obtained was purified by chromatography on silica gel using a cyclohexane/ethyl acetate mixture (80/20; v/v) as the eluent to give 9.1 g of the expected compound as a yellow solid (yield = 30%). mp = 67 °C. LC/MS (method b):  $R_t$  = 1.59 min. MS  $m/z$ : 238  $[M + H]^+$ .  $^1H$  NMR (300 MHz, DMSO- $d_6$ )  $\delta$  2.68 (m, 4H), 3.63 (s, 3H), 5.45 (s, 2H), 6.67 (dd,  $J$  = 8.3, 1.2 Hz, 1H), 7.02 (m, 2H).

Compounds **7b–d** were synthesized in a similar manner.

**Methyl 6-(2-Amino-5-chloro-phenyl)hex-5-ynoate (7b).** As described for **7a**, 4-chloro-2-iodo-nitrobenzene and methyl hex-5-ynoate were transformed to **6b**, which was reduced to **7b**, giving 41% yield. LC/MS (method b):  $R_t$  = 1.67 min. MS  $m/z$ : 252  $[M + H]^+$ .  $^1H$  NMR (250 MHz, DMSO- $d_6$ )  $\delta$  1.83 (m, 2H), 2.48 (m, 4H), 3.59 (s, 3H), 5.40 (s, 2H), 6.67 (d,  $J$  = 8.6 Hz, 1H), 7.03 (dd,  $J$  = 8.6, 2.4 Hz, 1H), 7.08 (d,  $J$  = 2.4 Hz, 1H).

**Methyl 7-(2-Amino-5-chloro-phenyl)hept-6-ynoate (7c).** As described for **7a**, 4-chloro-2-iodo-nitrobenzene and methyl hept-6-ynoate were transformed to **6c**, which was reduced to **7c**, giving a 68% yield. Yellow solid: mp = 66 °C. LC/MS (method b):  $R_t$  = 1.76 min. MS  $m/z$ : 264  $[M - H]^-$ .  $^1H$  NMR (400 MHz, DMSO- $d_6$ )  $\delta$  1.55 (m, 2H), 1.68 (m, 2H), 2.36 (t,  $J$  = 7.4 Hz, 2H), 2.47 (t,  $J$  = 7.0 Hz, 2H), 3.59 (s, 3H), 5.40 (s, 2H), 6.67 (d,  $J$  = 8.6 Hz, 1H), 7.03 (dd,  $J$  = 8.6, 2.6 Hz, 1H), 7.07 (d,  $J$  = 2.6 Hz, 1H).

**Methyl 6-(2-Amino-5-methoxy-phenyl)hex-5-ynoate (7d).** As described for **7a**, 2-iodo-4-methoxy-1-nitro-benzene and methyl hex-5-ynoate was transformed to **6d**, which was reduced to **7d**, giving a 40% yield. Brown oil.  $^1H$  NMR (300 MHz, DMSO- $d_6$ )  $\delta$  1.81 (m, 2H), 2.47 (t,  $J$  = 7.5 Hz, 2H), 2.48 (m, 2H), 3.60 (s, 3H), 3.62 (s, 3H), 4.80 (s, 2H), 6.62 (m, 1H), 6.68 (m, 2H).

**Methyl 6-[2-Amino-5-(trifluoromethyl)phenyl]hex-5-ynoate (7e).** As described for **7a**, 2-iodo-1-nitro-4-(trifluoromethyl)benzene and methyl hex-5-ynoate were transformed to **6e**, which was reduced to **7e**, giving a 50% yield. Brown oil.  $^1H$  NMR (300 MHz, DMSO- $d_6$ )  $\delta$  1.81 (m, 2H), 2.47 (t,  $J$  = 7.5 Hz, 2H), 2.48 (m, 2H), 3.60 (s, 3H), 5.98 (s, 2H), 6.78 (d, 1H), 7.31 (m, 2H).

**Methyl 5-[2-(Benzenesulfonamido)-5-chloro-phenyl]pent-4-ynoate (8a).** A solution of 1.2 g (5 mmol; 1 equiv) of **7a** in 15 mL of pyridine is prepared, and 0.77 mL (6 mmol; 1.2 equiv) of

benzenesulfonyl chloride was added. The mixture was stirred for 1 h at room temperature and then concentrated under reduced pressure. The residual oil was purified by chromatography on silica gel using a cyclohexane/ethyl acetate mixture (8/2; v/v) as the eluent to give 1.8 g of the expected compound as a beige solid (yield = 95%). LC/MS (method b):  $R_t$  = 1.82 min. MS  $m/z$ : 378  $[M + H]^+$ .  $^1H$  NMR (300 MHz, DMSO- $d_6$ )  $\delta$  2.56 (s, 4H), 3.65 (s, 3H), 7.28–7.36 (m, 3H), 7.54–7.72 (m, 5H), 9.69 (s, 1H).

Compounds **8b–m** were synthesized in a similar manner.

**Methyl 6-[2-(Benzenesulfonamido)-5-chloro-phenyl]hex-5-ynoate (8b).** Starting from **7b**, giving a 66% yield. Orange solid: mp = 90 °C. LC/MS (method b):  $R_t$  = 1.87 min. MS  $m/z$ : 390  $[M - H]^-$ .  $^1H$  NMR (400 MHz, DMSO- $d_6$ )  $\delta$  1.72 (m, 2H), 2.34 (t,  $J$  = 7.1 Hz, 2H), 2.43 (t,  $J$  = 7.4 Hz, 2H), 3.62 (s, 3H), 3.76 (d,  $J$  = 8.4 Hz, 1H), 7.36 (m, 2H), 7.54 (m, 2H), 7.63 (m, 1H), 7.69 (m, 2H).

**Methyl 7-[2-(Benzenesulfonamido)-5-chloro-phenyl]hept-6-ynoate (8c).** Starting from **7c**, giving a 54% yield. Colorless oil.  $^1H$  NMR (250 MHz, DMSO- $d_6$ )  $\delta$  1.55 (m, 4H), 2.33 (m, 4H), 3.60 (s, 3H), 7.22 (m, 3H), 7.61 (m, 5H), 9.75 (s, 1H).

**Methyl 6-[2-(Benzenesulfonamido)-5-methoxy-phenyl]hex-5-ynoate (8d).** Starting from **7d**, giving a 66% yield. Orange solid. LC/MS (method b):  $R_t$  = 1.66 min. MS  $m/z$ : 388  $[M + H]^+$ .  $^1H$  NMR (300 MHz, DMSO- $d_6$ )  $\delta$  1.70 (m, 2H), 2.29 (t,  $J$  = 7.1 Hz, 2H), 2.43 (t,  $J$  = 7.4 Hz, 2H), 3.62 (s, 3H), 3.70 (s, 3H), 6.78 (d,  $J$  = 2.9 Hz, 1H), 6.86 (dd,  $J$  = 8.9, 2.9 Hz, 1H), 7.12 (d,  $J$  = 8.9 Hz, 1H), 7.51 (m, 2H), 7.61 (m, 3H), 9.47 (s, 1H).

**Methyl 6-[2-(1,3-Benzodioxol-5-ylsulfonylamino)-5-chloro-phenyl]hex-5-ynoate (8e).** Starting from **7b** and 1,3-benzodioxole-5-sulfonyl chloride, giving a 89% yield. Brown oil. LC/MS (method a):  $R_t$  = 6.19 min. MS  $m/z$ : 436  $[M + H]^+$ .  $^1H$  NMR (300 MHz, DMSO- $d_6$ )  $\delta$  1.76 (m, 2H), 2.40 (t,  $J$  = 7.1 Hz, 2H), 2.44 (t,  $J$  = 7.3 Hz, 2H), 3.61 (s, 3H), 6.15 (s, 2H), 7.01 (m, 1H), 7.19 (m, 2H), 7.26 (m, 1H), 7.36 (m, 2H), 9.66 (s, 1H).

**Methyl 6-[5-Chloro-2-[(2-methyl-1,3-benzothiazol-6-yl)-sulfonylamino]phenyl]hex-5-ynoate (8h).** Starting from **7b** and 2-methyl-1,3-benzothiazole-6-sulfonyl chloride, giving a 68% yield. White solid. mp = 103–106 °C. LC/MS (method a):  $R_t$  = 6.17 min. MS  $m/z$ : 463  $[M + H]^+$ .  $^1H$  NMR (250 MHz, DMSO- $d_6$ )  $\delta$  1.63 (m, 2H), 2.26 (t,  $J$  = 7.8 Hz, 2H), 2.37 (t,  $J$  = 7.4 Hz, 2H), 2.83 (s, 3H), 3.61 (s, 3H), 7.29 (m, 3H), 7.73 (dd,  $J$  = 8.6, 1.8 Hz, 1H), 8.01 (d,  $J$  = 8.6 Hz, 1H), 8.42 (d,  $J$  = 1.8 Hz, 1H), 9.89 (s, 1H).

**Methyl 6-[5-Chloro-2-[(2-methyl-1,3-benzothiazol-5-yl)-sulfonylamino]phenyl]hex-5-ynoate (8i).** Starting from **7b** and 2-methyl-1,3-benzothiazole-5-sulfonyl chloride, giving a 42% yield. Yellow solid. mp = 68–72 °C. LC/MS (method a):  $R_t$  = 6.25 min. MS  $m/z$ : 463  $[M + H]^+$ .  $^1H$  NMR (250 MHz, DMSO- $d_6$ )  $\delta$  1.60 (m, 2H), 2.22 (t,  $J$  = 7.1 Hz, 2H), 2.35 (t,  $J$  = 7.4 Hz, 2H), 2.83 (s, 3H), 3.61 (s, 3H), 7.33 (m, 3H), 7.63 (dd,  $J$  = 8.5, 1.8 Hz, 1H), 8.15 (d,  $J$  = 1.6 Hz, 1H), 8.21 (d,  $J$  = 8.5 Hz, 1H), 9.94 (s, 1H).

**Methyl 6-[2-[(2-Amino-1,3-benzothiazol-6-yl)sulfonylamino]-5-chloro-phenyl]hex-5-ynoate (8j).** Starting from **7b** and 2-amino-1,3-benzothiazole-6-sulfonyl chloride, giving a 96% yield. Orange solid. mp = 60–65 °C. LC/MS (method a):  $R_t$  = 5.37 min. MS  $m/z$ : 464  $[M + H]^+$ .  $^1H$  NMR (250 MHz, DMSO- $d_6$ )  $\delta$  1.70 (m, 2H), 2.33 (t,  $J$  = 7.1 Hz, 2H), 2.42 (t,  $J$  = 7.4 Hz, 2H), 3.61 (m, 3H), 7.33 (m, 4H), 7.48 (dd,  $J$  = 8.8, 1.9 Hz, 1H), 7.96 (br. s, 2H), 8.04 (d,  $J$  = 1.9 Hz, 1H), 9.60 (s, 1H).

**Methyl 6-[2-[(2-Amino-1,3-benzoxazol-6-yl)sulfonylamino]-5-chloro-phenyl]hex-5-ynoate (8k).** Starting from **7b** and 2-amino-1,3-benzoxazole-6-sulfonyl chloride, giving a 9% yield. White solid. mp = 135 °C. LC/MS (method a):  $R_t$  = 5.22 min. MS  $m/z$ : 448  $[M + H]^+$ .  $^1H$  NMR (250 MHz, DMSO- $d_6$ )  $\delta$  1.70 (m, 2H), 2.33 (t,  $J$  = 7.1 Hz, 2H), 2.42 (t,  $J$  = 7.4 Hz, 2H), 3.61 (s, 3H), 7.29 (m, 4H), 7.45 (dd,  $J$  = 8.2, 1.8 Hz, 1H), 7.59 (d,  $J$  = 1.8 Hz, 1H), 7.86 (br. s, 2H), 9.57 (br. s, 1H).

**Methyl 6-[2-(2,1,3-Benzothiadiazol-5-ylsulfonylamino)-5-chloro-phenyl]hex-5-ynoate (8l).** Starting from **7b** and 2,1,3-benzothiadiazole-5-sulfonyl chloride, giving a 24% yield. Yellow oil. LC/MS (method a):  $R_t$  = 6.57 min. MS  $m/z$ : 450  $[M + H]^+$ .  $^1H$  NMR (300 MHz, DMSO- $d_6$ )  $\delta$  1.58 (m, 2H), 2.20 (t,  $J$  = 7.1 Hz, 2H),

2.33 (t,  $J = 7.4$  Hz, 2H), 3.60 (s, 3H), 7.35 (m, 3H), 7.92 (dd,  $J = 9.1$ , 1.8 Hz, 1H), 8.31 (d,  $J = 9.3$  Hz, 1H), 8.37 (m, 1H), 10.30 (s, 1H).

**Methyl 6-[2-(1,3-Benzothiazol-6-yl)sulfonylamino]-5-(trifluoromethyl)phenyl]hex-5-ynoate (8m).** Starting from **7e** and 1,3-benzothiazole-6-sulfonyl chloride, giving a 59% yield. Orange gum. LC/MS (method a):  $R_t = 6.15$  min. MS  $m/z$ : 483  $[M + H]^+$ .  $^1H$  NMR (250 MHz, DMSO- $d_6$ )  $\delta$  1.68 (m, 2H), 2.33 (t,  $J = 7.2$  Hz, 2H), 2.38 (d,  $J = 7.4$  Hz, 2H), 3.61 (s, 3H), 7.58 (m, 3H), 7.89 (dd,  $J = 8.6$ , 1.9 Hz, 1H), 8.24 (d,  $J = 8.6$  Hz, 1H), 8.69 (d,  $J = 1.9$  Hz, 1H), 9.62 (s, 1H), 10.22 (br. s, 1H).

**Methyl 3-[1-(Benzenesulfonyl)-5-chloro-indol-2-yl]propanoate (9a).** A solution of 300 mg (0.79 mmol; 1 equiv) of **8a** in 35 mL of 1,2-dichloroethane was prepared, 15 mg (0.08 mmol; 0.1 equiv) of copper acetate was added, and the mixture was refluxed for 24 h, with stirring. The solvent was then driven off under reduced pressure, and the residual viscous solid was purified by chromatography on silica gel using a toluene/ethyl acetate mixture (9/1; v/v) as the eluent to give 230 mg of the compound obtained as a yellow solid (yield = 77%). mp = 93–96 °C. LC/MS (method b):  $R_t = 1.92$  min. no ionization.  $^1H$  NMR (500 MHz, DMSO- $d_6$ )  $\delta$  2.81 (t,  $J = 7.4$  Hz, 2H), 3.28 (t,  $J = 7.1$  Hz, 2H), 3.61 (s, 3H), 6.60 (s, 1H), 7.32 (dd,  $J = 8.9$ , 2.2 Hz, 1H), 7.58 (m, 3H), 7.71 (m, 1H), 7.82 (d,  $J = 8.5$  Hz, 2H), 8.02 (d,  $J = 8.9$  Hz, 1H).

Compounds **9b–c** were synthesized in a similar manner.

**Methyl 4-[1-(Benzenesulfonyl)-5-chloro-indol-2-yl]butanoate (9b).** Starting from **8b**, giving an 81% yield. White solid: mp = 109–112 °C. LC/MS (method b):  $R_t = 2.01$  min. MS  $m/z$ : 390  $[M - H]^-$ .  $^1H$  NMR (400 MHz, DMSO- $d_6$ )  $\delta$  1.96 (m, 2H), 2.43 (t,  $J = 7.4$  Hz, 2H), 3.02 (t,  $J = 7.1$  Hz, 2H), 3.59 (s, 3H), 6.62 (s, 1H), 7.32 (dd,  $J = 8.8$ , 2.2 Hz, 1H), 7.58 (m, 3H), 7.70 (m, 1H), 7.80 (m, 2H), 8.04 (d,  $J = 9.0$  Hz, 1H).

**Methyl 5-[1-(Benzenesulfonyl)-5-chloro-indol-2-yl]pentanoate (9c).** Starting from **8c**, giving a 75% yield. Beige solid: mp = 95–98 °C. LC/MS (method b):  $R_t = 2.09$  min. MS  $m/z$ : 406  $[M + H]^+$ .  $^1H$  NMR (400 MHz, DMSO- $d_6$ )  $\delta$  1.63 (m, 2H), 1.70 (m, 2H), 2.36 (t,  $J = 7.3$  Hz, 2H), 2.99 (t,  $J = 6.9$  Hz, 2H), 3.59 (s, 3H), 6.61 (s, 1H), 7.31 (dd,  $J = 9.0$ , 2.2 Hz, 1H), 7.57 (m, 3H), 7.70 (m, 1H), 7.81 (d,  $J = 8.6$  Hz, 2H), 8.04 (d,  $J = 9.0$  Hz, 1H).

**Methyl 4-[1-(Benzenesulfonyl)-5-methoxy-indol-2-yl]butanoate (9d).** A solution of 1.14 g (2.95 mmol; 1 equiv) of **8d** in 10 mL of 1,2-dichloroethane was prepared, 540 mg (2.98 mmol; 1.01 equiv) of copper acetate was added, and the mixture was heated at 150 °C under microwave for 30 min, with stirring. The reaction mixture was filtered, and the residue was evaporated to give 1.06 g of a brown solid (yield = 93%). Brown solid: mp = 80–82 °C. LC/MS (method a):  $R_t = 6.15$  min. MS  $m/z$ : 388  $[M + H]^+$ .  $^1H$  NMR (300 MHz, DMSO- $d_6$ )  $\delta$  1.96 (m, 2H), 2.42 (t,  $J = 7.4$  Hz, 2H), 3.00 (t,  $J = 7.5$  Hz, 2H), 3.59 (s, 3H), 3.74 (s, 3H), 6.55 (s, 1H), 6.88 (dd,  $J = 9.1$ , 2.7 Hz, 1H), 7.00 (d,  $J = 2.7$  Hz, 1H), 7.54 (m, 2H), 7.65 (m, 1H), 7.74 (m, 2H), 7.91 (d,  $J = 9.1$  Hz, 1H).

Compounds **9e–m** were synthesized in a similar manner.

**Methyl 4-[1-(1,3-Benzodioxol-5-yl)sulfonyl]-5-chloro-indol-2-yl]butanoate (9e).** Starting from **8e**, giving a 97% yield. White solid. mp = 97–103 °C. LC/MS (method a):  $R_t = 6.71$  min. MS  $m/z$ : 436  $[M + H]^+$ .  $^1H$  NMR (300 MHz, DMSO- $d_6$ )  $\delta$  1.96 (m, 2H), 2.44 (t,  $J = 7.4$  Hz, 2H), 3.02 (t,  $J = 7.3$  Hz, 2H), 3.59 (s, 3H), 6.14 (s, 2H), 6.60 (s, 1H), 7.04 (d,  $J = 8.3$  Hz, 1H), 7.27 (d,  $J = 2.1$  Hz, 1H), 7.30 (dd,  $J = 9.0$ , 2.2 Hz, 1H), 7.42 (dd,  $J = 8.3$ , 2.1 Hz, 1H), 7.58 (d,  $J = 2.2$  Hz, 1H), 8.03 (d,  $J = 9.0$  Hz, 1H).

**Methyl 4-[5-Chloro-1-(2-naphthylsulfonyl)indol-2-yl]butanoate (9f).** As described for **8a**, naphthalene-2-sulfonyl chloride was reacted with **7b** to give **8f**, which was used crude in the next step. Compound **9f** was then obtained with a 71% yield. White solid. mp = 116–118 °C. LC/MS (method b):  $R_t = 2.19$  min. MS  $m/z$ : 440  $[M - H]^-$ .  $^1H$  NMR (400 MHz, DMSO- $d_6$ )  $\delta$  1.98 (m, 2H), 2.45 (t,  $J = 7.4$  Hz, 2H), 3.10 (t,  $J = 7.4$  Hz, 2H), 3.57 (s, 3H), 6.62 (m, 1H), 7.31 (dd,  $J = 9.0$ , 2.2 Hz, 1H), 7.57 (d,  $J = 2.0$  Hz, 1H), 7.63 (dd,  $J = 8.8$ , 2.0 Hz, 1H), 7.72 (m, 2H), 8.00 (d,  $J = 9.0$  Hz, 1H), 8.06 (d,  $J = 9.0$  Hz, 1H), 8.12 (d,  $J = 9.0$  Hz, 1H), 8.23 (d,  $J = 9.0$  Hz, 1H), 8.72 (d,  $J = 2.0$  Hz, 1H).

**Methyl 4-[5-Chloro-1-(1-naphthylsulfonyl)indol-2-yl]butanoate (9g).** As described for **8a**, naphthalene-1-sulfonyl chloride was reacted with **7b** to give **8g**, which was used crude in the next step. Compound **9g** was then obtained with a 44% yield. White solid. mp = 94–97 °C. LC/MS (method b):  $R_t = 2.17$  min. MS  $m/z$ : 440  $[M - H]^-$ .  $^1H$  NMR (400 MHz, DMSO- $d_6$ )  $\delta$  1.86 (m, 2H), 2.35 (t,  $J = 7.4$  Hz, 2H), 2.89 (t,  $J = 7.4$  Hz, 2H), 3.53 (s, 3H), 6.70 (s, 1H), 7.30 (dd,  $J = 8.8$ , 2.2 Hz, 1H), 7.65 (m, 5H), 7.94 (d,  $J = 9.2$  Hz, 1H), 8.13 (m, 1H), 8.34 (m, 2H).

**Methyl 4-[5-Chloro-1-[(2-methyl-1,3-benzothiazol-6-yl)sulfonyl]indol-2-yl]butanoate (9h).** Starting from **8h**, giving a 74% yield. White solid. mp = 151–153 °C. LC/MS (method a):  $R_t = 6.95$  min. MS  $m/z$ : 463  $[M + H]^+$ .  $^1H$  NMR (300 MHz, DMSO- $d_6$ )  $\delta$  1.96 (m, 2H), 2.44 (t,  $J = 7.4$  Hz, 2H), 2.83 (s, 3H), 3.07 (t,  $J = 7.3$  Hz, 2H), 3.58 (s, 3H), 6.61 (s, 1H), 7.31 (dd,  $J = 9.0$ , 2.2 Hz, 1H), 7.57 (d,  $J = 2.2$  Hz, 1H), 7.78 (dd,  $J = 8.8$ , 2.0 Hz, 1H), 8.01 (d,  $J = 8.8$  Hz, 1H), 8.08 (d,  $J = 8.8$  Hz, 1H), 8.81 (d,  $J = 2.0$  Hz, 1H).

**Methyl 4-[5-Chloro-1-[(2-methyl-1,3-benzothiazol-5-yl)sulfonyl]indol-2-yl]butanoate (9i).** Starting from **8i**, giving a 77% yield. Beige solid. mp = 136–138 °C. LC/MS (method a):  $R_t = 6.92$  min. MS  $m/z$ : 463  $[M + H]^+$ .  $^1H$  NMR (250 MHz, DMSO- $d_6$ )  $\delta$  1.98 (m, 2H), 2.45 (t,  $J = 7.3$  Hz, 2H), 2.81 (s, 3H), 3.08 (t,  $J = 7.5$  Hz, 2H), 3.59 (s, 3H), 6.62 (s, 1H), 7.32 (dd,  $J = 8.9$ , 2.2 Hz, 1H), 7.57 (d,  $J = 1.9$  Hz, 1H), 7.75 (dd,  $J = 8.5$ , 1.9 Hz, 1H), 8.11 (d,  $J = 8.9$  Hz, 1H), 8.26 (m, 2H).

**Methyl 4-[1-[(2-Amino-1,3-benzothiazol-6-yl)sulfonyl]-5-chloro-indol-2-yl]butanoate (9j).** Starting from **8j**, giving a 43% yield. Yellow solid. mp = 235–239 °C. LC/MS (method b):  $R_t = 1.80$  min. MS  $m/z$ : 464  $[M + H]^+$ .  $^1H$  NMR (250 MHz, DMSO- $d_6$ )  $\delta$  1.96 (m, 2H), 2.44 (t,  $J = 7.4$  Hz, 2H), 3.05 (t,  $J = 7.5$  Hz, 2H), 3.59 (s, 3H), 6.58 (s, 1H), 7.31 (m, 2H), 7.60 (m, 2H), 8.06 (m, 3H), 8.31 (m, 1H).

**Methyl 4-[1-[(2-Amino-1,3-benzoxazol-6-yl)sulfonyl]-5-chloro-indol-2-yl]butanoate (9k).** Starting from **8k**, giving a 46% yield. Yellow solid. mp = 238 °C. LC/MS (method a):  $R_t = 5.79$  min. MS  $m/z$ : 448  $[M + H]^+$ .  $^1H$  NMR (250 MHz, DMSO- $d_6$ )  $\delta$  1.97 (m, 2H), 2.44 (t,  $J = 7.5$  Hz, 2H), 3.05 (t,  $J = 7.4$  Hz, 2H), 3.59 (s, 3H), 6.58 (s, 1H), 7.27 (m, 2H), 7.55 (m, 2H), 7.83 (s, 1H), 8.06 (m, 3H).

**Methyl 4-[1-(2,1,3-Benzothiadiazol-5-yl)sulfonyl]-5-chloro-indol-2-yl]butanoate (9l).** Starting from **8l**, giving an 83% yield. Yellow solid. mp = 103–106 °C. LC/MS (method a):  $R_t = 6.97$  min. MS  $m/z$ : 450  $[M + H]^+$ .  $^1H$  NMR (300 MHz, DMSO- $d_6$ )  $\delta$  1.98 (m, 2H), 2.46 (t,  $J = 7.4$  Hz, 2H), 3.10 (t,  $J = 7.3$  Hz, 2H), 3.58 (s, 3H), 6.67 (s, 1H), 7.34 (dd,  $J = 8.9$ , 2.2 Hz, 1H), 7.59 (d,  $J = 1.9$  Hz, 1H), 7.81 (dd,  $J = 9.2$ , 1.9 Hz, 1H), 8.13 (d,  $J = 8.9$  Hz, 1H), 8.25 (d,  $J = 9.2$  Hz, 1H), 8.81 (m, 1H).

**Methyl 4-[1-(1,3-Benzothiazol-6-yl)sulfonyl]-5-(trifluoromethyl)indol-2-yl]butanoate (9m).** Starting from **8m**, giving a 49% yield. White solid. mp = 116–121 °C.  $^1H$  NMR (300 MHz, DMSO- $d_6$ )  $\delta$  1.99 (m, 2H), 2.47 (t,  $J = 7.7$  Hz, 2H), 3.11 (t,  $J = 7.4$  Hz, 2H), 3.58 (s, 3H), 6.78 (s, 1H), 7.63 (d,  $J = 8.8$  Hz, 1H), 7.89 (dd,  $J = 8.8$ , 2.1 Hz, 1H), 7.93 (s, 1H), 8.22 (d,  $J = 8.8$  Hz, 1H), 8.30 (d,  $J = 8.8$  Hz, 1H), 9.02 (d,  $J = 2.1$  Hz, 1H), 9.66 (s, 1H).

Compounds **10b–m** were synthesized in a similar manner as compound **4**.

**4-[1-(Benzenesulfonyl)-5-chloro-indol-2-yl]butanoic Acid (10b).** Starting from **9b**, giving a 92% yield. Pale pink solid: mp = 198–202 °C. LC/MS (method b):  $R_t = 1.77$  min. MS  $m/z$ : 376  $[M - H]^-$ .  $^1H$  NMR (400 MHz, DMSO- $d_6$ )  $\delta$  1.93 (m, 2H), 2.33 (t,  $J = 7.2$  Hz, 2H), 3.03 (t,  $J = 7.5$  Hz, 2H), 6.62 (s, 1H), 7.31 (dd,  $J = 9.0$ , 2.0 Hz, 1H), 7.57 (m, 3H), 7.70 (m, 1H), 7.81 (d,  $J = 7.5$  Hz, 2H), 8.04 (d,  $J = 9.0$  Hz, 1H), 12.10 (br. s, 1H).  $^{13}C$  NMR (126 MHz, DMSO- $d_6$ )  $\delta$  174.1, 143.1, 137.4, 134.8, 134.7, 131.0, 129.9, 128.3, 126.1, 123.9, 120.0, 115.7, 108.7, 33.0, 27.6, 23.5.

**5-[1-(Benzenesulfonyl)-5-chloro-indol-2-yl]pentanoic Acid (10c).** Starting from **9c**, giving a 79% yield. White solid: mp = 144–148 °C. LC/MS (method b):  $R_t = 1.80$  min. MS  $m/z$ : 390  $[M - H]^-$ .  $^1H$  NMR (400 MHz, DMSO- $d_6$ )  $\delta$  1.60 (m, 2H), 1.70 (m, 2H), 2.27 (t,  $J = 7.3$  Hz, 2H), 2.99 (t,  $J = 7.1$  Hz, 2H), 6.61 (s, 1H), 7.31 (dd,  $J = 8.9$ , 2.3 Hz, 1H), 7.58 (m, 3H), 7.70 (m, 1H), 7.81 (m, 2H), 8.04



(d,  $J$  = 9.0 Hz, 1H), 12.03 (br. s, 1H).  $^{13}\text{C}$  NMR (101 MHz, DMSO- $d_6$ )  $\delta$  174.3, 143.4, 137.4, 134.8, 134.7, 131.0, 129.9, 128.2, 126.1, 123.9, 119.9, 115.7, 108.6, 33.3, 28.0, 27.8, 24.1.

**4-[1-(Benzenesulfonyl)-5-methoxy-indol-2-yl]butanoic Acid (10d).** Starting from **9d**, giving a 94% yield. White solid. LC/MS (method a):  $R_t$  = 5.26 min. MS  $m/z$ : 374  $[\text{M} + \text{H}]^+$ .  $^1\text{H}$  NMR (250 MHz, DMSO- $d_6$ )  $\delta$  1.94 (m, 2H), 2.32 (t,  $J$  = 7.1 Hz, 2H), 3.00 (t,  $J$  = 7.2 Hz, 2H), 3.74 (s, 3H), 6.54 (s, 1H), 6.88 (dd,  $J$  = 9.1, 2.7 Hz, 1H), 7.00 (d,  $J$  = 2.7 Hz, 1H), 7.54 (m, 2H), 7.65 (m, 1H), 7.75 (m, 2H), 7.91 (d,  $J$  = 9.1 Hz, 1H), 12.06 (br. s, 1H).  $^{13}\text{C}$  NMR (75 MHz, DMSO- $d_6$ )  $\delta$  174.1, 156.2, 141.9, 137.5, 134.4, 130.7, 130.6, 129.7, 126.0, 115.1, 112.5, 109.8, 103.2, 55.2, 32.9, 27.7, 23.7.

**4-[1-(1,3-Benzodioxol-5-ylsulfonyl)-5-chloro-indol-2-yl]butanoic Acid (10e).** Starting from **9e**, giving a 96% yield. White solid. mp = 154–156 °C. LC/MS (method a):  $R_t$  = 5.87 min. MS  $m/z$ : 420  $[\text{M} - \text{H}]^-$ .  $^1\text{H}$  NMR (250 MHz, DMSO- $d_6$ )  $\delta$  1.93 (m, 2H), 2.35 (t,  $J$  = 6.6 Hz, 2H), 3.03 (t,  $J$  = 7.6 Hz, 2H), 6.14 (s, 2H), 6.60 (s, 1H), 7.04 (d,  $J$  = 8.2 Hz, 1H), 7.29 (m, 2H), 7.43 (dd,  $J$  = 8.2, 2.1 Hz, 1H), 7.58 (d,  $J$  = 1.9 Hz, 1H), 8.03 (d,  $J$  = 8.9 Hz, 1H), 12.11 (br. s, 1H).  $^{13}\text{C}$  NMR (75 MHz, DMSO- $d_6$ )  $\delta$  174.1, 152.6, 148.2, 143.0, 134.6, 130.9, 130.2, 128.1, 123.8, 122.7, 119.8, 115.7, 108.7, 108.4, 105.8, 103.0, 32.9, 27.6, 23.5.

**4-[5-Chloro-1-(2-naphthylsulfonyl)indol-2-yl]butanoic Acid (10f).** Starting from **9f**, giving a 90% yield. White solid. mp = 166–169 °C. LC/MS (method b):  $R_t$  = 1.96 min. MS  $m/z$ : 426  $[\text{M} - \text{H}]^-$ .  $^1\text{H}$  NMR (400 MHz, DMSO- $d_6$ )  $\delta$  1.95 (m, 2H), 2.36 (t,  $J$  = 7.4 Hz, 2H), 3.11 (t,  $J$  = 7.5 Hz, 2H), 6.61 (s, 1H), 7.31 (dd,  $J$  = 9.0, 2.2 Hz, 1H), 7.56 (d,  $J$  = 2.0 Hz, 1H), 7.72 (m, 3H), 8.00 (d,  $J$  = 7.9 Hz, 1H), 8.06 (d,  $J$  = 9.02 Hz, 1H), 8.12 (d,  $J$  = 9.02 Hz, 1H), 8.23 (d,  $J$  = 7.9 Hz, 1H), 8.72 (d,  $J$  = 1.8 Hz, 1H), 12.19 (s, 1H).  $^{13}\text{C}$  NMR (101 MHz, DMSO- $d_6$ )  $\delta$  174.2, 143.1, 134.8, 134.7, 134.3, 131.4, 130.9, 130.2, 129.9, 129.7, 128.2, 128.2, 128.1, 127.9, 123.9, 120.6, 119.9, 115.7, 108.6, 33.0, 27.7, 23.6.

**4-[5-Chloro-1-(1-naphthylsulfonyl)indol-2-yl]butanoic Acid (10g).** Starting from **9g**, giving an 89% yield. White solid. mp = 206–210 °C. LC/MS (method b):  $R_t$  = 1.94 min. MS  $m/z$ : 426  $[\text{M} - \text{H}]^-$ .  $^1\text{H}$  NMR (500 MHz, DMSO- $d_6$ )  $\delta$  1.84 (m, 2H), 2.26 (t,  $J$  = 7.3 Hz, 2H), 2.90 (t,  $J$  = 7.5 Hz, 2H), 6.70 (s, 1H), 7.30 (dd,  $J$  = 8.9, 2.2 Hz, 1H), 7.61 (m, 2H), 7.69 (m, 3H), 7.93 (d,  $J$  = 8.9 Hz, 1H), 8.13 (m, 1H), 8.35 (m, 2H), 12.09 (br. s, 1H).  $^{13}\text{C}$  NMR (101 MHz, DMSO- $d_6$ )  $\delta$  174.0, 143.4, 135.7, 135.2, 134.0, 133.8, 130.3, 129.5, 129.0, 128.1, 127.8, 127.6, 127.0, 124.7, 123.9, 122.7, 120.2, 115.4, 107.8, 32.9, 27.3, 23.2.

**4-[5-Chloro-1-[(2-methyl-1,3-benzothiazol-6-yl)sulfonyl]indol-2-yl]butanoic Acid (10h).** Starting from **9h**, giving an 85% yield. White solid. mp = 163–165 °C. LC/MS (method b):  $R_t$  = 1.78 min. MS  $m/z$ : 447  $[\text{M} - \text{H}]^-$ .  $^1\text{H}$  NMR (300 MHz, DMSO- $d_6$ )  $\delta$  1.94 (m, 2H), 2.35 (t,  $J$  = 7.3 Hz, 2H), 2.82 (s, 3H), 3.08 (t,  $J$  = 7.2 Hz, 2H), 6.61 (s, 1H), 7.31 (dd,  $J$  = 9.0, 2.2 Hz, 1H), 7.57 (d,  $J$  = 2.2 Hz, 1H), 7.78 (dd,  $J$  = 8.7, 2.1 Hz, 1H), 8.01 (d,  $J$  = 8.7 Hz, 1H), 8.08 (d,  $J$  = 9.0 Hz, 1H), 8.82 (d,  $J$  = 2.1 Hz, 1H), 12.11 (s, 1H).  $^{13}\text{C}$  NMR (101 MHz, DMSO- $d_6$ )  $\delta$  174.1, 173.9, 156.2, 143.0, 136.2, 134.7, 133.1, 130.9, 128.2, 123.9, 123.5, 122.9, 122.2, 119.9, 115.7, 108.6, 32.9, 27.7, 23.6, 20.1.

**4-[5-Chloro-1-[(2-methyl-1,3-benzothiazol-5-yl)sulfonyl]indol-2-yl]butanoic Acid (10i).** Starting from **9i**, giving a 98% yield. White solid. mp = 164 °C. LC/MS (method a):  $R_t$  = 6.01 min. MS  $m/z$ : 447  $[\text{M} - \text{H}]^-$ .  $^1\text{H}$  NMR (300 MHz, DMSO- $d_6$ )  $\delta$  1.94 (m, 2H), 2.35 (t,  $J$  = 7.3 Hz, 2H), 2.81 (s, 3H), 3.08 (t,  $J$  = 7.5 Hz, 2H), 6.62 (s, 1H), 7.32 (dd,  $J$  = 8.8, 2.0 Hz, 1H), 7.57 (d,  $J$  = 2.0 Hz, 1H), 7.75 (dd,  $J$  = 8.8, 2.0 Hz, 1H), 8.10 (d,  $J$  = 8.8 Hz, 1H), 8.25 (d,  $J$  = 8.8 Hz, 1H), 8.28 (d,  $J$  = 2.0 Hz, 1H), 12.14 (br. s, 1H).  $^{13}\text{C}$  NMR (101 MHz, DMSO- $d_6$ )  $\delta$  174.1, 171.6, 152.2, 143.1, 141.8, 135.1, 134.8, 131.0, 128.3, 124.0, 124.0, 121.2, 120.0, 119.5, 115.8, 108.9, 32.9, 27.7, 23.6, 19.9.

**4-[1-[(2-Amino-1,3-benzothiazol-6-yl)sulfonyl]-5-chloro-indol-2-yl]butanoic Acid (10j).** Starting from **9j**, giving a 49% yield. White solid. mp = 155–162 °C. LC/MS (method b):  $R_t$  = 1.55 min. MS  $m/z$ : 448  $[\text{M} - \text{H}]^-$ .  $^1\text{H}$  NMR (250 MHz, DMSO- $d_6$ )  $\delta$  1.93 (m, 2H), 2.35 (t,  $J$  = 6.7 Hz, 2H), 3.06 (t,  $J$  = 7.4 Hz, 2H), 4.28 (br. s, 2H), 6.58 (s, 1H), 7.29 (dd,  $J$  = 8.9, 2.0 Hz, 1H), 7.36 (d,  $J$  = 8.6 Hz, 1H), 7.56

(d,  $J$  = 2.0 Hz, 1H), 7.62 (dd,  $J$  = 8.6, 2.0 Hz, 1H), 8.05 (d,  $J$  = 8.9 Hz, 1H), 8.27 (br. s, 1H), 8.33 (d,  $J$  = 2.0 Hz, 1H).  $^{13}\text{C}$  NMR (101 MHz, DMSO- $d_6$ )  $\delta$  174.2, 171.1, 154.0 (broad), 143.1, 134.7, 131.0, 130.5 (broad), 129.4, 128.1, 124.7, 123.8, 121.0, 119.9, 116.7, 115.8, 108.3, 33.1, 27.7, 23.6.

**4-[1-[(2-Amino-1,3-benzoxazol-6-yl)sulfonyl]-5-chloro-indol-2-yl]butanoic Acid (10k).** Starting from **9k**, giving a 76% yield. Yellow solid. mp = 220 °C. LC/MS (method a):  $R_t$  = 5.03 min. MS  $m/z$ : 432  $[\text{M} - \text{H}]^-$ .  $^1\text{H}$  NMR (250 MHz, DMSO- $d_6$ )  $\delta$  1.93 (m, 2H), 2.35 (t,  $J$  = 7.0 Hz, 2H), 3.05 (t,  $J$  = 8.4 Hz, 2H), 6.57 (s, 1H), 7.26 (d,  $J$  = 9.0 Hz, 1H), 7.30 (dd,  $J$  = 9.0, 2.2 Hz, 1H), 7.55 (m, 2H), 7.83 (d,  $J$  = 2.2 Hz, 1H), 8.03 (s, 2H), 8.07 (d,  $J$  = 9.0 Hz, 1H), 12.09 (s, 1H).

**4-[1-(2,1,3-Benzothiadiazol-5-ylsulfonyl)-5-chloro-indol-2-yl]butanoic Acid (10l).** Starting from **9l**, giving a 92% yield. Brown solid. mp = 172–175 °C. LC/MS (method a):  $R_t$  = 6.03 min. MS  $m/z$ : 434  $[\text{M} - \text{H}]^-$ .  $^1\text{H}$  NMR (300 MHz, DMSO- $d_6$ )  $\delta$  1.95 (m, 2H), 2.28–2.41 (t,  $J$  = 7.7 Hz, 2H), 3.10 (t,  $J$  = 7.4 Hz, 2H), 6.67 (s, 1H), 7.33 (dd,  $J$  = 8.9, 2.2 Hz, 1H), 7.59 (d,  $J$  = 2.2 Hz, 1H), 7.81 (dd,  $J$  = 9.3, 2.0 Hz, 1H), 8.13 (d,  $J$  = 8.9 Hz, 1H), 8.20–8.29 (m, 1H), 8.82 (d,  $J$  = 2.0 Hz, 1H), 12.10 (br. s, 1H).  $^{13}\text{C}$  NMR (101 MHz, DMSO- $d_6$ )  $\delta$  174.2, 155.4, 152.4, 143.1, 137.9, 134.7, 131.0, 128.5, 124.2, 124.1, 123.9, 121.8, 120.1, 115.8, 109.1, 32.9, 27.7, 23.6.

**4-[1-(1,3-Benzothiazol-6-ylsulfonyl)-5-(trifluoromethyl)indol-2-yl]butanoic Acid (10m).** Starting from **9m**, giving a 97% yield. Yellow solid. mp = 173–181 °C. LC/MS (method a):  $R_t$  = 5.79 min. MS  $m/z$ : 467  $[\text{M} - \text{H}]^-$ .  $^1\text{H}$  NMR (250 MHz, DMSO- $d_6$ )  $\delta$  1.96 (m, 2H), 2.38 (t,  $J$  = 7.3 Hz, 2H), 3.12 (t,  $J$  = 7.4 Hz, 2H), 6.78 (s, 1H), 7.62 (dd,  $J$  = 8.8, 1.6 Hz, 1H), 7.91 (m, 2H), 8.22 (d,  $J$  = 8.8 Hz, 1H), 8.30 (d,  $J$  = 8.8 Hz, 1H), 9.02 (d,  $J$  = 1.6 Hz, 1H), 9.66 (s, 1H), 12.12 (br. s, 1H).  $^{13}\text{C}$  NMR (126 MHz, DMSO- $d_6$ )  $\delta$  174.1, 162.7, 156.2, 143.4, 137.9, 134.8, 133.9, 129.4, 124.6 (q,  $J_{\text{C,F}}$  = 272.2 Hz), 124.4 (q,  $J_{\text{C,F}}$  = 31.7 Hz), 124.3, 123.5, 123.1, 120.6 (q,  $J_{\text{C,F}}$  = 2.7 Hz), 117.9 (q,  $J_{\text{C,F}}$  = 2.7 Hz), 114.9, 109.0, 32.9, 27.6, 23.5.

**N-(4-Chloro-2-iodo-phenyl)benzenesulfonamide (11a).** A solution of 2 g (7.89 mmol; 1 equiv) of 4-chloro-2-iodoaniline in 30 mL of pyridine was prepared, and 1.21 mL (9.5 mmol; 1.2 equiv) of benzenesulfonyl chloride was added at 0 °C, with stirring. The reaction mixture was subsequently stirred at room temperature for 16 h and then concentrated under reduced pressure. The residual oil was taken up with 50 mL of ethyl acetate, and the solution obtained was washed with water and then dried over magnesium sulfate and concentrated under reduced pressure. The crude product was therefore taken up in solution in 60 mL of dioxane and treated with 19 mL of 3 M potassium hydroxide solution under gentle reflux for 8 h. The solvent was driven off under reduced pressure, and the residue was taken up with water and acidified to pH 2 with dilute hydrochloric acid solution. The precipitate was filtered off, washed with water, and dried to give 2.79 g of the expected product as a white solid (yield = 90%). mp = 126–128 °C. LC/MS (method b):  $R_t$  = 1.75 min. MS  $m/z$ : 392  $[\text{M} - \text{H}]^-$ .  $^1\text{H}$  NMR (300 MHz, DMSO- $d_6$ )  $\delta$  7.00 (d,  $J$  = 8.6 Hz, 1H), 7.40 (dd,  $J$  = 8.6, 2.5 Hz, 1H), 7.59 (m, 2H), 7.68 (m, 3H), 7.89 (d,  $J$  = 2.5 Hz, 1H), 9.88 (s, 1H).

**N-(2-Iodo-4-methyl-phenyl)benzenesulfonamide (11c).** This compound was prepared as described in the case of **11a**, starting from 2-bromo-4-methyl-aniline and benzenesulfonyl chloride, giving a 95% yield. Beige solid: LC/MS (method a):  $R_t$  = 5.46 min. MS  $m/z$ : 326  $[\text{M} + \text{H}]^+$ .  $^1\text{H}$  NMR (250 MHz, DMSO- $d_6$ )  $\delta$  2.25 (s, 3H), 7.03 (d,  $J$  = 8.2 Hz, 1H), 7.13 (m, 1H), 7.41 (d,  $J$  = 1.4 Hz, 1H), 7.58 (m, 2H), 7.69 (m, 3H), 9.77 (s, 1H).

**N-(4-Chloro-2-iodo-phenyl)-4-methyl-2,3-dihydro-1,4-benzoxazine-6-sulfonamide (11d).** This compound was prepared as described in the case of **8a**, starting from 4-chloro-2-iodo-aniline and 4-methyl-2,3-dihydro-1,4-benzoxazine-6-sulfonyl chloride, giving a 80% yield. Beige solid. mp = 159 °C. LC/MS (method b):  $R_t$  = 1.81 min. MS  $m/z$ : 465  $[\text{M} + \text{H}]^+$ .  $^1\text{H}$  NMR (300 MHz, DMSO- $d_6$ )  $\delta$  2.80 (s, 3H), 3.28 (m, 2H), 4.29 (m, 2H), 6.79 (d,  $J$  = 9.5 Hz, 1H), 6.92 (m, 2H), 7.03 (d,  $J$  = 8.8 Hz, 1H), 7.41 (dd,  $J$  = 8.8, 2.6 Hz, 1H), 7.89 (d,  $J$  = 2.6 Hz, 1H), 9.50 (s, 1H).

**N-(4-Chloro-2-iodo-phenyl)-1,3-benzothiazole-6-sulfonamide (11e).** This compound was prepared as described in the case of **8a**,

starting from 4-chloro-2-iodo-aniline and 1,3-benzothiazole-6-sulfonyl chloride, giving a 60% yield. Yellow solid. mp = 184 °C. LC/MS (method a):  $R_t$  = 5.47 min. MS  $m/z$ : 450  $[M + H]^+$ .  $^1H$  NMR (300 MHz, DMSO- $d_6$ )  $\delta$  7.03 (d,  $J$  = 8.4 Hz, 1H), 7.31 (dd,  $J$  = 8.8, 2.6 Hz, 1H), 7.82 (m, 2H), 8.22 (d,  $J$  = 8.8 Hz, 1H), 8.58 (d,  $J$  = 1.8 Hz, 1H), 9.59 (s, 1H), 9.95 (br. s, 1H).

**Methyl 2-[[1-(Benzenesulfonyl)-5-chloro-indol-2-yl]methoxy]acetate (12a).** A mixture of 600 mg (1.52 mmol; 1 equiv) of 11a and 0.5 mL of dimethylformamide was prepared in a microwave reaction tube, and 14 mg (0.02 mmol; 0.013 equiv) of cuprous iodide, 27 mg (0.04 mmol; 0.026 equiv) of bis(triphenylphosphine)-dichloropalladium, 293 mg (2.29 mmol; 1.5 equiv) of the methyl ester of (2-propynyloxy)acetic acid, and, finally, 0.5 mL of diethylamine were added. The mixture was heated by microwave at 130 °C for 15 min and then cooled and hydrolyzed with water. The mixture was extracted three times with ethyl acetate, and the combined organic phases were washed with water and then dried over magnesium sulfate and concentrated under reduced pressure. The residue was purified by chromatography on silica gel using a cyclohexane/ethyl acetate mixture (90/10; v/v) as the eluent to give 0.42 g of the expected compound as a yellow solid (yield = 71%). mp = 98–100 °C. LC/MS (method a):  $R_t$  = 6.36 min. MS  $m/z$ : 416  $[MNa]^+$ .  $^1H$  NMR (250 MHz, DMSO- $d_6$ )  $\delta$  3.68 (s, 3H), 4.25 (s, 2H), 4.97 (s, 2H), 6.88 (s, 1H), 7.37 (dd,  $J$  = 8.9, 2.2 Hz, 1H), 7.57 (m, 2H), 7.70 (m, 2H), 8.00 (m, 3H).

Compounds 12c–e were synthesized in a similar manner.

**Methyl 4-[1-(Benzenesulfonyl)-5-methyl-indol-2-yl]butanoate (12c).** Starting from 11c and methyl hex-5-ynoate, giving a 36% yield. LC/MS (method a):  $R_t$  = 6.64 min. MS  $m/z$ : 372  $[M + H]^+$ .  $^1H$  NMR (250 MHz, DMSO- $d_6$ )  $\delta$  1.98 (m, 2H), 2.35 (s, 3H), 2.43 (m, 2H), 3.02 (t,  $J$  = 7.4 Hz, 2H), 3.61 (s, 3H), 6.55 (s, 1H), 7.11 (dd,  $J$  = 8.5, 1.4 Hz, 1H), 7.28 (s, 1H), 7.55 (m, 2H), 7.66 (m, 1H), 7.76 (m, 2H), 7.91 (d,  $J$  = 8.5 Hz, 1H).

**Methyl 4-[5-Chloro-1-[(4-methyl-2,3-dihydro-1,4-benzoxazin-6-yl)sulfonyl]indol-2-yl]butanoate (12d).** Starting from 11d and methyl hex-5-ynoate, giving a 90% yield. White solid. mp = 139–140 °C. LC/MS (method b):  $R_t$  = 2.08 min. MS  $m/z$ : 463  $[M + H]^+$ .  $^1H$  NMR (300 MHz, DMSO- $d_6$ )  $\delta$  1.96 (m, 2H), 2.43 (t,  $J$  = 7.3 Hz, 2H), 2.77 (s, 3H), 3.02 (t,  $J$  = 7.5 Hz, 2H), 3.24 (m, 2H), 3.59 (s, 3H), 4.23 (m, 2H), 6.58 (s, 1H), 6.76 (d,  $J$  = 8.4 Hz, 1H), 6.87 (d,  $J$  = 2.2 Hz, 1H), 7.00 (dd,  $J$  = 8.4, 2.2 Hz, 1H), 7.30 (dd,  $J$  = 8.8, 2.2 Hz, 1H), 7.57 (d,  $J$  = 2.2 Hz, 1H), 8.06 (d,  $J$  = 8.8 Hz, 1H).

**Methyl 4-[1-(1,3-Benzothiazol-6-ylsulfonyl)-5-chloro-indol-2-yl]butanoate (12e).** Starting from 11e and methyl hex-5-ynoate, giving a quantitative yield. White solid. LC/MS (method a):  $R_t$  = 6.52 min. MS  $m/z$ : 449  $[M + H]^+$ .  $^1H$  NMR (500 MHz, DMSO- $d_6$ )  $\delta$  1.97 (m, 2H), 2.51 (t,  $J$  = 7.3 Hz, 2H), 3.08 (t,  $J$  = 7.4 Hz, 2H), 3.58 (s, 3H), 6.63 (s, 1H), 7.32 (dd,  $J$  = 8.9, 2.2 Hz, 1H), 7.58 (d,  $J$  = 2.2 Hz, 1H), 7.84 (dd,  $J$  = 8.8, 2.0 Hz, 1H), 8.09 (d,  $J$  = 8.9 Hz, 1H), 8.20 (d,  $J$  = 8.8 Hz, 1H), 8.97 (d,  $J$  = 2.0 Hz, 1H), 9.65 (s, 1H).

**2-[[1-(Benzenesulfonyl)-5-chloro-indol-2-yl]methoxy]acetic Acid (13a).** This compound was prepared as described in the case of 4, starting from 12a, giving a 98% yield. White solid: mp = 140–142 °C. LC/MS (method a):  $R_t$  = 5.61 min. MS  $m/z$ : 378  $[M - H]^-$ .  $^1H$  NMR (300 MHz, DMSO- $d_6$ )  $\delta$  4.14 (s, 2H), 4.96 (s, 2H), 6.87 (s, 1H), 7.36 (dd,  $J$  = 9.0, 2.2 Hz, 1H), 7.57 (m, 2H), 7.70 (m, 2H), 8.01 (m, 3H), 12.79 (br. s, 1H).  $^{13}C$  NMR (75 MHz, DMSO- $d_6$ )  $\delta$  171.2, 138.7, 137.1, 134.8, 134.5, 130.2, 129.7, 128.3, 126.7, 124.7, 120.7, 115.5, 110.8, 67.0, 65.2.

**4-[1-(Benzenesulfonyl)-5-chloro-indol-2-yl]-2,2-dimethyl-butanoic Acid (13b).** This compound was prepared as described in the case of 12a, starting from 11a and 2,2-dimethyl-5-hexynoic acid, giving a 32% yield. Brown solid: mp = 242 °C. LC/MS (method a):  $R_t$  = 6.52 min. MS  $m/z$ : 404  $[M - H]^-$ .  $^1H$  NMR (250 MHz, DMSO- $d_6$ )  $\delta$  1.20 (s, 6H), 1.90 (m, 2H), 2.95 (m, 2H), 6.63 (s, 1H), 7.33 (dd,  $J$  = 8.8, 2.2 Hz, 1H), 7.59 (m, 3H), 7.76 (m, 3H), 8.06 (d,  $J$  = 8.8 Hz, 1H), 12.26 (s, 1H).  $^{13}C$  NMR (101 MHz, DMSO- $d_6$ )  $\delta$  178.4, 143.5, 137.4, 134.8, 134.7, 131.0, 130.0, 128.2, 126.0, 123.9, 119.9, 115.7, 108.4, 41.2, 38.7, 24.9, 24.2.

**4-[1-(Benzenesulfonyl)-5-methyl-indol-2-yl]butanoic Acid (13c).** This compound was prepared as described in the case of 4, starting from

12c, giving a 7% yield. Beige solid. LC/MS (method a):  $R_t$  = 5.67 min. MS  $m/z$ : 356  $[M - H]^-$ .  $^1H$  NMR (500 MHz, DMSO- $d_6$ )  $\delta$  2.04 (m, 2H), 2.34 (s, 3H), 2.51 (m, 2H), 3.01 (m, 2H), 6.52 (s, 1H), 7.10 (d,  $J$  = 8.5 Hz, 1H), 7.27 (s, 1H), 7.56 (m, 2H), 7.67 (s, 1H), 7.76 (m, 2H), 7.90 (d,  $J$  = 8.5 Hz, 1H), 12.12 (s, 1H).

**4-[5-Chloro-1-[(4-methyl-2,3-dihydro-1,4-benzoxazin-6-yl)sulfonyl]indol-2-yl]butanoic Acid (13d).** This compound was prepared as described in the case of 4, starting from 12d, giving an 80% yield. White solid. mp = 164–166 °C. LC/MS (method b):  $R_t$  = 1.84 min. MS  $m/z$ : 447  $[M - H]^-$ .  $^1H$  NMR (300 MHz, DMSO- $d_6$ )  $\delta$  1.93 (m, 2H), 2.33 (t,  $J$  = 7.1 Hz, 2H), 2.78 (s, 3H), 3.02 (t,  $J$  = 7.5 Hz, 2H), 3.24 (m, 2H), 4.23 (m, 2H), 6.57 (s, 1H), 6.76 (d,  $J$  = 8.4 Hz, 1H), 6.88 (d,  $J$  = 2.2 Hz, 1H), 7.01 (dd,  $J$  = 8.4, 2.2 Hz, 1H), 7.30 (dd,  $J$  = 8.8, 2.2 Hz, 1H), 7.57 (d,  $J$  = 2.2 Hz, 1H), 8.06 (d,  $J$  = 8.8 Hz, 1H), 12.41 (br. s, 1H).  $^{13}C$  NMR (101 MHz, DMSO- $d_6$ )  $\delta$  174.1, 148.5, 143.1, 137.1, 134.9, 130.9, 129.6, 127.9, 123.6, 119.8, 115.9, 115.8, 115.7, 108.3, 108.1, 64.7, 47.1, 37.8, 33.0, 27.6, 23.5.

**tert-Butyl 6-[2-Amino-5-(trifluoromethyl)phenyl]hex-5-ynoate (14a).** This compound was prepared as described in the case of 12a, starting from 2-iodo-4-(trifluoromethyl)aniline and tert-butyl hex-5-ynoate, giving a 64% yield. Brown solid. LC/MS (method a):  $R_t$  = 6.92 min. MS  $m/z$ : 328  $[M + H]^+$ .  $^1H$  NMR (250 MHz, DMSO- $d_6$ )  $\delta$  1.40 (s, 9H), 1.78 (t,  $J$  = 7.3 Hz, 2H), 2.36 (t,  $J$  = 7.3 Hz, 2H), 2.50 (m, 2H), 5.98 (s, 2H), 6.78 (d,  $J$  = 8.5 Hz, 1H), 7.31 (dd,  $J$  = 8.7, 2.0 Hz, 1H), 7.36 (d,  $J$  = 2.0 Hz, 1H).

**tert-Butyl 6-(2-Amino-5-chloro-phenyl)hex-5-ynoate (14b).** This compound was prepared as described in the case of 12a, starting from 4-chloro-2-iodo-aniline and tert-butyl hex-5-ynoate, giving a 95% yield. Brown oil. LC/MS (method a):  $R_t$  = 6.93 min. MS  $m/z$ : 294  $[M + H]^+$ .  $^1H$  NMR (250 MHz, DMSO- $d_6$ )  $\delta$  1.40 (s, 9H), 1.77 (m, 2H), 2.35 (t,  $J$  = 7.3 Hz, 2H), 2.49 (t,  $J$  = 7.7 Hz, 2H), 5.40 (s, 2H), 6.68 (d,  $J$  = 8.6 Hz, 1H), 7.04 (dd,  $J$  = 8.6, 2.3 Hz, 1H), 7.09 (d,  $J$  = 2.3 Hz, 1H).

**tert-Butyl 4-[5-(Trifluoromethyl)-1H-indol-2-yl]butanoate (15a).** This compound was prepared as described in the case of 9d, starting from 14a, giving a 68% yield. Brown solid. LC/MS (method b):  $R_t$  = 2.05 min. MS  $m/z$ : 326  $[M - H]^-$ .  $^1H$  NMR (300 MHz, DMSO- $d_6$ )  $\delta$  1.39 (s, 9H), 1.91 (m, 2H), 2.25 (t,  $J$  = 7.5 Hz, 2H), 2.76 (t,  $J$  = 7.5 Hz, 2H), 6.32 (s, 1H), 7.29 (d,  $J$  = 8.6 Hz, 1H), 7.45 (d,  $J$  = 8.6 Hz, 1H), 7.80 (s, 1H), 11.39 (s, 1H).

**tert-Butyl 4-(5-Chloro-1H-indol-2-yl)butanoate (15b).** This compound was prepared as described in the case of 9a, starting from 14b, giving a 64% yield. Brown solid. LC/MS (method b):  $R_t$  = 2.02 min. MS  $m/z$ : 292  $[M - H]^-$ .  $^1H$  NMR (250 MHz, DMSO- $d_6$ )  $\delta$  1.39 (s, 9H), 1.89 (m, 2H), 2.24 (t,  $J$  = 7.4 Hz, 2H), 2.72 (t,  $J$  = 7.5 Hz, 2H), 6.13 (d,  $J$  = 1.4 Hz, 1H), 6.98 (dd,  $J$  = 8.6, 2.1 Hz, 1H), 7.27 (d,  $J$  = 8.6 Hz, 1H), 7.44 (d,  $J$  = 2.1 Hz, 1H), 11.11 (br. s, 1H).

**4-[1-(Benzenesulfonyl)-5-(trifluoromethyl)indol-2-yl]butanoic Acid (16a).** To a solution of 115 mg (0.35 mmol; 1 equiv) of 15a in 0.5 mL of dimethylformamide was added at 0 °C 28 mg (0.7 mmol; 2 equiv) of sodium hydride, and the reaction mixture was stirred 2 min at room temperature. Benzenesulfonyl chloride (123 mg, 0.7 mmol; 2 equiv) in solution in 0.7 mL of dimethylformamide was added, and the reaction mixture was stirred 24 h at room temperature and then poured into a mixture of ice and saturated  $NH_4Cl$  solution. The mixture obtained was extracted with ethyl acetate; the combined organic phases were dried over magnesium sulfate and concentrated under reduced pressure. The residue was dissolved in 0.8 mL of dichloromethane and 0.2 mL of trifluoroacetic acid and stirred at room temperature for 5 h. The solvents were evaporated, and the residue was purified by HPLC using an acetonitrile/water gradient mixture as the eluent to give the expected compound as a beige solid (yield = 43%). mp = 209 °C. LC/MS (method b):  $R_t$  = 1.81 min. MS  $m/z$ : 410  $[M - H]^-$ .  $^1H$  NMR (400 MHz, DMSO- $d_6$ )  $\delta$  1.95 (m, 2H), 2.35 (t,  $J$  = 7.4 Hz, 2H), 3.06 (t,  $J$  = 7.3 Hz, 2H), 6.77 (s, 1H), 7.60 (m, 3H), 7.71 (m, 1H), 7.86 (d,  $J$  = 8.5 Hz, 2H), 7.94 (m, 1H), 8.25 (d,  $J$  = 8.8 Hz, 1H), 12.17 (br. s, 1H).  $^{13}C$  NMR (126 MHz, DMSO- $d_6$ )  $\delta$  174.1, 143.4, 138.0, 137.4, 134.9, 130.1, 129.4, 126.2, 124.5 (q, JCF = 272.8 Hz), 124.4 (q, JCF = 31.6 Hz), 120.6 (q, JCF = 3.5 Hz), 117.9 (q, JCF = 4.0 Hz), 114.9, 109.0, 32.9, 27.6, 23.5.

Compounds 16b–j were synthesized in a similar manner.



4-[1-(3-Methoxyphenyl)sulfonyl-5-(trifluoromethyl)indol-2-yl]butanoic Acid (**16b**). Starting from **15a** and 3-methoxybenzenesulfonyl chloride, giving a 46% yield. White solid. LC/MS (method b):  $R_t = 1.85$  min. MS  $m/z$ : 440  $[M - H]^-$ .  $^1H$  NMR (500 MHz, DMSO- $d_6$ )  $\delta$  1.95 (m, 2H), 2.36 (t,  $J = 7.3$  Hz, 2H), 3.06 (t,  $J = 7.4$  Hz, 2H), 3.77 (s, 3H), 6.78 (s, 1H), 7.28 (m, 2H), 7.38 (m, 1H), 7.50 (m, 1H), 7.63 (dd,  $J = 8.9, 1.6$  Hz, 1H), 7.94 (s, 1H), 8.25 (d,  $J = 9.2$  Hz, 1H), 12.15 (br. s, 1H).  $^{13}C$  NMR (126 MHz, DMSO- $d_6$ )  $\delta$  174.1, 159.6, 143.5, 138.5, 138.0, 131.4, 129.4, 124.6 (q, JCF = 271.8 Hz), 124.4 (q, JCF = 31.8 Hz), 120.6 (q, JCF = 3.3 Hz), 120.5, 118.1, 117.9 (q, JCF = 4.0 Hz), 114.9, 111.1, 109.1, 55.7, 32.9, 27.5, 23.5.

4-[1-(4-Methoxyphenyl)sulfonyl-5-(trifluoromethyl)indol-2-yl]butanoic Acid (**16c**). Starting from **15a** and 4-methoxybenzenesulfonyl chloride, giving a 48% yield. White solid. LC/MS (method b):  $R_t = 1.83$  min. MS  $m/z$ : 440  $[M - H]^-$ .  $^1H$  NMR (500 MHz, DMSO- $d_6$ )  $\delta$  1.94 (m, 2H), 2.35 (t,  $J = 7.3$  Hz, 2H), 3.06 (t,  $J = 7.4$  Hz, 2H), 3.79 (s, 3H), 6.74 (s, 1H), 7.07 (d,  $J = 8.9$  Hz, 2H), 7.61 (dd,  $J = 8.9, 1.7$  Hz, 1H), 7.81 (d,  $J = 8.9$  Hz, 2H), 7.93 (m, 1H), 8.25 (d,  $J = 8.9$  Hz, 1H), 12.17 (br. s, 1H).  $^{13}C$  NMR (126 MHz, DMSO- $d_6$ )  $\delta$  174.1, 163.9, 143.4, 137.9, 129.3, 128.8, 128.7, 124.6 (q, JCF = 271.8 Hz), 124.2 (q, JCF = 31.4 Hz), 120.4 (q, JCF = 3.3 Hz), 117.8 (q, JCF = 3.9 Hz), 115.1, 114.9, 108.7, 55.8, 32.9, 27.6, 23.5.

4-[1-(2-Methoxyphenyl)sulfonyl-5-(trifluoromethyl)indol-2-yl]butanoic Acid (**16d**). Starting from **15a** and 2-methoxybenzenesulfonyl chloride, giving a 3% yield. White solid. LC/MS (method b):  $R_t = 1.78$  min. MS  $m/z$ : 440  $[M - H]^-$ .  $^1H$  NMR (500 MHz, DMSO- $d_6$ )  $\delta$  1.93 (m, 2H), 2.32 (m, 2H), 2.98 (m, 2H), 3.52 (s, 3H), 6.69 (s, 1H), 7.14 (d,  $J = 8.2$  Hz, 1H), 7.19 (m, 1H), 7.52 (dd,  $J = 8.7, 1.5$  Hz, 1H), 7.68 (m, 1H), 7.93 (m, 2H), 8.07 (dd,  $J = 8.0, 1.5$  Hz, 1H), 12.13 (br. s, 1H).

4-[1-(3-Chlorophenyl)sulfonyl-5-(trifluoromethyl)indol-2-yl]butanoic Acid (**16e**). Starting from **15a** and 3-chlorobenzenesulfonyl chloride, giving a 16% yield. White solid. LC/MS (method b):  $R_t = 1.91$  min. MS  $m/z$ : 444  $[M - H]^-$ .  $^1H$  NMR (500 MHz, DMSO- $d_6$ )  $\delta$  1.95 (m, 2H), 2.36 (t,  $J = 7.3$  Hz, 2H), 3.07 (t,  $J = 7.3$  Hz, 2H), 6.81 (s, 1H), 7.62 (m, 2H), 7.80 (m, 2H), 7.93 (t,  $J = 1.9$  Hz, 1H), 7.95 (m, 1H), 8.24 (d,  $J = 8.8$  Hz, 1H), 12.17 (br. s, 1H).  $^{13}C$  NMR (126 MHz, DMSO- $d_6$ )  $\delta$  174.1, 143.5, 139.0, 137.9, 135.0, 134.5, 132.1, 129.5, 125.7, 125.0, 124.6 (q, JCF = 31.7 Hz), 124.5 (q, JCF = 272.0 Hz), 120.8 (q, JCF = 3.1 Hz), 118.0 (q, JCF = 3.8 Hz), 114.9, 109.4, 32.9, 27.5, 23.5.

4-[1-(4-Chlorophenyl)sulfonyl-5-(trifluoromethyl)indol-2-yl]butanoic Acid (**16f**). Starting from **15a** and 4-chlorobenzenesulfonyl chloride, giving a 36% yield. White solid. LC/MS (method a):  $R_t = 6.45$  min. MS  $m/z$ : 446  $[M + H]^+$ .  $^1H$  NMR (500 MHz, DMSO- $d_6$ )  $\delta$  1.94 (m, 2H), 2.35 (t,  $J = 7.3$  Hz, 2H), 3.04 (t,  $J = 7.3$  Hz, 2H), 6.79 (s, 1H), 7.64 (m, 3H), 7.87 (m, 2H), 7.95 (s, 1H), 8.23 (d,  $J = 8.8$  Hz, 1H), 12.19 (br. s, 1H).  $^{13}C$  NMR (75 MHz, DMSO- $d_6$ )  $\delta$  174.1, 143.3, 139.9, 137.9, 136.1, 130.2, 129.4, 128.2, 124.6 (q, JCF = 32.0 Hz), 124.5 (q, JCF = 271.4 Hz), 120.7, 118.0, 114.8, 109.3, 32.9, 27.5, 23.5.

4-[1-(2-Chlorophenyl)sulfonyl-5-(trifluoromethyl)indol-2-yl]butanoic Acid (**16g**). Starting from **15a** and 2-chlorobenzenesulfonyl chloride, giving a 9% yield. White solid. LC/MS (method b):  $R_t = 1.86$  min. MS  $m/z$ : 444  $[M - H]^-$ .  $^1H$  NMR (500 MHz, DMSO- $d_6$ )  $\delta$  1.86 (m, 2H), 2.29 (t,  $J = 7.1$  Hz, 2H), 2.92 (t,  $J = 7.5$  Hz, 2H), 6.82 (s, 1H), 7.56 (dd,  $J = 8.9, 1.3$  Hz, 1H), 7.64 (m, 1H), 7.70 (dd,  $J = 8.5, 1.5$  Hz, 1H), 7.76 (m, 1H), 7.94 (d,  $J = 8.8$  Hz, 1H), 8.02 (m, 2H), 12.10 (br. s, 1H).  $^{13}C$  NMR (126 MHz, DMSO- $d_6$ )  $\delta$  173.9, 144.3, 138.1, 136.4, 135.7, 132.6, 131.2, 130.9, 128.8, 128.5, 124.6 (q, JCF = 272.6 Hz), 124.2 (q, JCF = 32.2 Hz), 120.4 (q, JCF = 3.4 Hz), 118.1 (q, JCF = 3.8 Hz), 114.5, 107.9, 32.9, 27.3, 23.2.

4-[1-(3-(Trifluoromethoxy)phenyl)sulfonyl-5-(trifluoromethyl)indol-2-yl]butanoic Acid (**16h**). Starting from **15a** and 3-(trifluoromethoxy)benzenesulfonyl chloride, giving a 21% yield. White solid. LC/MS (method b):  $R_t = 1.98$  min. MS  $m/z$ : 494  $[M - H]^-$ .  $^1H$  NMR (500 MHz, DMSO- $d_6$ )  $\delta$  1.94 (m, 2H), 2.34 (t,  $J = 7.3$  Hz, 2H), 3.06 (t,  $J = 7.4$  Hz, 2H), 6.80 (s, 1H), 7.63 (dd,  $J = 8.8, 1.7$  Hz, 1H), 7.74 (m, 2H), 7.84 (s, 1H), 7.88 (dt,  $J = 7.2, 1.8$  Hz, 1H), 7.94 (s, 1H), 8.26 (d,  $J = 8.8$  Hz, 1H), 12.21 (br. s, 1H).  $^{13}C$  NMR (126 MHz, DMSO- $d_6$ )  $\delta$  174.1, 148.3, 143.5, 138.9, 138.0, 132.7, 129.6, 127.6,

125.4, 124.8 (q, JCF = 31.9 Hz), 124.5 (q, JCF = 272.2 Hz), 120.8 (q, JCF = 3.3 Hz), 119.7 (q, JCF = 258.9 Hz), 119.0, 118.0 (q, JCF = 3.9 Hz), 115.0, 109.7, 32.9, 27.6, 23.5.

4-[1-(4-(Trifluoromethoxy)phenyl)sulfonyl-5-(trifluoromethyl)indol-2-yl]butanoic Acid (**16i**). Starting from **15a** and 4-(trifluoromethoxy)benzenesulfonyl chloride, giving a 16% yield. White solid. LC/MS (method b):  $R_t = 1.99$  min. MS  $m/z$ : 494  $[M - H]^-$ .  $^1H$  NMR (500 MHz, DMSO- $d_6$ )  $\delta$  1.94 (m, 2H), 2.34 (t,  $J = 7.3$  Hz, 2H), 3.05 (t,  $J = 7.3$  Hz, 2H), 6.80 (s, 1H), 7.57 (d,  $J = 9.0$  Hz, 2H), 7.64 (dd,  $J = 8.9, 1.65$  Hz, 1H), 7.96 (s, 1H), 8.02 (d,  $J = 9.0$  Hz, 2H), 8.24 (d,  $J = 8.9$  Hz, 1H), 12.13 (br. s, 1H).  $^{13}C$  NMR (126 MHz, DMSO- $d_6$ )  $\delta$  174.1, 152.3, 143.3, 137.9, 136.0, 129.5, 129.2, 124.6 (q, JCF = 31.7 Hz), 124.5 (q, JCF = 271.7 Hz), 121.9, 120.8 (q, JCF = 3.3 Hz), 119.6 (q, JCF = 259.4 Hz), 118.0 (q, JCF = 4.0 Hz), 114.8, 109.3, 32.9, 27.5, 23.5.

4-[5-Chloro-1-(3-methoxyphenyl)sulfonyl-indol-2-yl]butanoic Acid (**16j**). Starting from **15b** and 3-methoxybenzenesulfonyl chloride, giving a 25% yield. White solid. LC/MS (method b):  $R_t = 1.81$  min. MS  $m/z$ : 406  $[M - H]^-$ .  $^1H$  NMR (400 MHz, DMSO- $d_6$ )  $\delta$  1.93 (m, 2H), 2.34 (t,  $J = 7.4$  Hz, 2H), 3.02 (t,  $J = 7.4$  Hz, 2H), 3.76 (s, 3H), 6.63 (s, 1H), 7.22 (m, 1H), 7.26 (m, 1H), 7.33 (m, 2H), 7.49 (t,  $J = 9.5$  Hz, 1H), 7.59 (d,  $J = 2.2$  Hz, 1H), 8.04 (d,  $J = 10.1$  Hz, 1H), 12.12 (br. s, 1H).  $^{13}C$  NMR (75 MHz, DMSO- $d_6$ )  $\delta$  174.1, 159.5, 143.1, 138.5, 134.8, 131.3, 131.0, 128.3, 123.9, 120.3, 119.9, 118.0, 115.7, 111.0, 108.7, 55.7, 32.9, 27.6, 23.5.

4-[5-Chloro-1-(4-methoxyphenyl)sulfonyl-indol-2-yl]butanoic Acid (**16k**). Starting from **15b** and 4-methoxybenzenesulfonyl chloride, giving a 26% yield. White solid. LC/MS (method b):  $R_t = 1.80$  min. MS  $m/z$ : 406  $[M - H]^-$ .  $^1H$  NMR (400 MHz, DMSO- $d_6$ )  $\delta$  1.93 (m, 2H), 2.34 (t,  $J = 7.3$  Hz, 2H), 3.02 (t,  $J = 7.3$  Hz, 2H), 3.79 (s, 3H), 6.59 (s, 1H), 7.06 (d,  $J = 9.0$  Hz, 2H), 7.30 (dd,  $J = 8.9, 2.3$  Hz, 1H), 7.57 (d,  $J = 2.3$  Hz, 1H), 7.76 (d,  $J = 9.0$  Hz, 2H), 8.04 (d,  $J = 8.9$  Hz, 1H), 12.14 (br. s, 1H).  $^{13}C$  NMR (75 MHz, DMSO- $d_6$ )  $\delta$  174.1, 163.7, 143.0, 134.7, 130.9, 128.8, 128.6, 128.1, 123.8, 119.8, 115.7, 115.0, 108.4, 55.8, 32.9, 27.6, 23.5.

4-[5-Chloro-1-(*m*-tolylsulfonyl)indol-2-yl]butanoic Acid (**16l**). Starting from **15b** and 3-methylbenzenesulfonyl chloride, giving a 25% yield. White solid. LC/MS (method a):  $R_t = 5.53$  min. MS  $m/z$ : 392  $[M + H]^+$ .  $^1H$  NMR (500 MHz, DMSO- $d_6$ )  $\delta$  1.93 (m, 2H), 2.33 (m, 5H), 3.03 (t,  $J = 7.4$  Hz, 2H), 6.61 (s, 1H), 7.31 (dd,  $J = 8.9, 2.2$  Hz, 1H), 7.44 (m, 1H), 7.50 (m, 1H), 7.57 (m, 2H), 7.67 (s, 1H), 8.03 (d,  $J = 8.9$  Hz, 1H), 12.20 (br. s, 1H).  $^{13}C$  NMR (101 MHz, DMSO- $d_6$ )  $\delta$  174.1, 143.1, 140.0, 137.4, 135.4, 134.7, 130.9, 129.7, 128.2, 126.2, 123.9, 123.3, 119.9, 115.7, 108.5, 33.0, 27.6, 23.5, 20.7.

4-[5-Chloro-1-(*p*-tolylsulfonyl)indol-2-yl]butanoic Acid (**16m**). Starting from **15b** and 4-methylbenzenesulfonyl chloride, giving an 11% yield. White solid. LC/MS (method a):  $R_t = 5.53$  min. MS  $m/z$ : 392  $[M + H]^+$ .  $^1H$  NMR (500 MHz, DMSO- $d_6$ )  $\delta$  1.92 (m, 2H), 2.32 (s, 3H), 2.33 (t,  $J = 7.7$  Hz, 2H), 3.02 (t,  $J = 7.4$  Hz, 2H), 6.59 (s, 1H), 7.30 (dd,  $J = 8.9, 2.2$  Hz, 1H), 7.36 (d,  $J = 8.5$  Hz, 2H), 7.57 (d,  $J = 2.2$  Hz, 1H), 7.70 (d,  $J = 8.5$  Hz, 2H), 8.03 (d,  $J = 8.9$  Hz, 1H), 12.18 (br. s, 1H).

**Methyl 6-[5-Chloro-2-[(4-fluoro-3-nitro-phenyl)sulfonylamino]phenyl]hex-5-ynoate (17)**. To a solution of 1.4 g of 4-fluoro-3-nitro-benzenesulfonyl chloride (5.9 mmol; 1.48 equiv) in 10 mL of dichloromethane was added 0.5 mL of pyridine (5.9 mmol; 1.48 equiv) and 49 mg of dimethylaminopyridine (0.37 mmol; 0.09 equiv), and the reaction mixture was cooled to 0 °C. Then, 1 g of **7b** (3.97 mmol; 1 equiv) was added slowly, and the reaction mixture was stirred at room temperature for 18 h. Dichloromethane was added, and the mixture was washed successively with 1 N solution of HCl, water, and saturated solution of NaCl. The organic layer was dried on magnesium sulfate and evaporated. The residue was purified by chromatography on silica gel using a toluene/ethyl acetate mixture (95/5; v/v) as the eluent to give 1.8 g of expected compound (quantitative yield). LC/MS (method a):  $R_t = 6.32$  min. MS  $m/z$ : 455  $[M + H]^+$ .  $^1H$  NMR (300 MHz, DMSO- $d_6$ )  $\delta$  1.70 (m, 2H), 2.32 (t,  $J = 7.7$  Hz, 2H), 2.41 (t,  $J = 7.3$  Hz, 2H), 3.60 (s, 3H), 7.26 (m, 1H), 7.40 (m, 2H), 7.80 (m, 1H), 8.03 (m, 1H), 8.38 (m, 1H), 10.31 (s, 1H).

**Methyl 4-[5-Chloro-1-(4-fluoro-3-nitro-phenyl)sulfonyl-indol-2-yl]butanoate (18).** This compound was prepared as described in the case of **9d**, starting from **17**, giving a 96% yield. Yellow solid. mp = 93 °C. LC/MS (method a):  $R_t$  = 6.76 min. MS  $m/z$ : 455  $[M + H]^+$ .  $^1H$  NMR (300 MHz, DMSO- $d_6$ )  $\delta$  1.97 (m, 2H), 2.45 (t,  $J$  = 7.3 Hz, 2H), 3.03 (t,  $J$  = 7.5 Hz, 2H), 3.59 (s, 3H), 6.70 (s, 1H), 7.36 (m, 1H), 7.63 (m, 1H), 7.78 (m, 1H), 8.06 (d,  $J$  = 9.1 Hz, 1H), 8.19 (m, 1H), 8.47 (m, 1H).

**Methyl 4-[1-(4-Amino-3-nitro-phenyl)sulfonyl-5-chloro-indol-2-yl]butanoate (19).** To a solution of 100 mg of **18** in (0.220 mmol; 1 equiv) in 1 mL of dioxane was added 0.77 mL of a 30% aqueous ammonia solution, and the reaction mixture was stirred 30 min at room temperature. Ethyl acetate was added, and the mixture was washed successively with water and a saturated solution of NaCl. The organic layer was dried on magnesium sulfate and evaporated to give 100 mg of the expected compound as a yellow solid (quantitative yield). LC/MS (method b):  $R_t$  = 1.91 min. MS  $m/z$ : 450  $[M - H]^-$ .  $^1H$  NMR (250 MHz, DMSO- $d_6$ )  $\delta$  1.96 (m, 2H), 2.44 (t,  $J$  = 7.4 Hz, 2H), 3.01 (t,  $J$  = 7.4 Hz, 2H), 3.60 (s, 3H), 6.63 (s, 1H), 7.05 (d,  $J$  = 9.0 Hz, 1H), 7.34 (dd,  $J$  = 8.8, 2.2 Hz, 1H), 7.62 (m, 2H), 8.02 (d,  $J$  = 8.8 Hz, 1H), 8.16 (br. s, 2H), 8.37 (d,  $J$  = 2.2 Hz, 1H).

**Methyl 4-[5-Chloro-1-(3,4-diaminophenyl)sulfonyl-indol-2-yl]butanoate (20).** To a suspension of 604 mg of **19** (1.33 mmol; 1 equiv) in 8 mL of acetic acid was added 394 mg of iron (6.65 mmol; 5 equiv), and the reaction mixture was stirred at 60 °C for 2 h. The reaction mixture was filtered, and the solid was rinsed with water. The solution was extracted with ethyl acetate. The obtained organic layer was washed with a saturated NaCl solution, dried on magnesium sulfate, and evaporated to give 566 mg of the expected compound as a pale yellow solid. (Quantitative yield). LC/MS (method a):  $R_t$  = 5.74 min. MS  $m/z$ : 422  $[M + H]^+$ .  $^1H$  NMR (250 MHz, DMSO- $d_6$ )  $\delta$  1.96 (m, 2H), 2.44 (t,  $J$  = 7.3 Hz, 2H), 3.01 (t,  $J$  = 7.4 Hz, 2H), 3.61 (s, 3H), 4.94 (s, 2H), 5.58 (s, 2H), 6.48 (d,  $J$  = 8.2 Hz, 1H), 6.53 (s, 1H), 6.90 (m, 2H), 7.27 (dd,  $J$  = 8.8, 2.0 Hz, 1H), 7.56 (d,  $J$  = 2.0 Hz, 1H), 8.01 (d,  $J$  = 8.8 Hz, 1H).

**Methyl 4-[1-(1H-Benzimidazol-5-yl)sulfonyl]-5-chloro-indol-2-yl]butanoate (21).** A suspension of 87 mg of **20** (0.20 mmol; 1 equiv) in 0.21 mL of formic acid was stirred 2 h at 100 °C for 2 h. At room temperature, a 1 N NaOH solution was added, and the mixture was extracted twice with ethyl acetate. The combined organic layers were washed successively with water and a saturated NaCl solution, then dried on magnesium sulfate and evaporated to give 73 mg of the expected compound as a yellow oil (yield: 82%). LC/MS (method a):  $R_t$  = 5.68 min. MS  $m/z$ : 432  $[M + H]^+$ .  $^1H$  NMR (300 MHz, DMSO- $d_6$ )  $\delta$  1.97 (m, 2H), 2.44 (t,  $J$  = 7.3 Hz, 2H), 3.06 (t,  $J$  = 7.3 Hz, 2H), 3.59 (s, 3H), 6.59 (s, 1H), 7.20 (m, 1H), 7.32 (dd,  $J$  = 8.9, 2.4 Hz, 1H), 7.58 (m, 2H), 7.72 (d,  $J$  = 8.0 Hz, 1H), 8.11 (m, 2H), 8.47 (s, 1H).

**4-[1-(1H-Benzimidazol-5-yl)sulfonyl]-5-chloro-indol-2-yl]butanoic Acid (22).** This compound was prepared as described in the case of **4**, starting from **21**, giving a 66% yield. White solid. mp = 212 °C. LC/MS (method a):  $R_t$  = 5.02 min. MS  $m/z$ : 416  $[M - H]^-$ .  $^1H$  NMR (250 MHz, DMSO- $d_6$ )  $\delta$  1.95 (m, 2H), 2.34 (t,  $J$  = 7.9 Hz, 2H), 3.08 (t,  $J$  = 7.4 Hz, 2H), 6.59 (s, 1H), 7.32 (dd,  $J$  = 8.8, 2.2 Hz, 1H), 7.59 (m, 2H), 7.73 (d,  $J$  = 8.8 Hz, 1H), 8.11 (m, 2H), 8.47 (s, 1H), 12.61 (br. s, 1H).  $^{13}C$  NMR (101 MHz, DMSO- $d_6$ )  $\delta$  174.5, 146.1, 143.2, 134.9, 131.0, 130.5, 129.8, 128.1, 128.0, 123.8, 119.9, 119.6, 115.8, 108.4, 33.3, 27.8, 23.7, 1 unobserved carbon.

**PPAR Transactivation Assays.** These cell-based assays were carried out using Cos-7 cells transfected with a chimeric human or murine PPAR $\alpha$ -Gal4 receptor expression plasmid (or PPAR $\delta$ -Gal4, or PPAR $\gamma$ -Gal4) and a 5Gal4 pGL3 TK Luc reporter plasmid. Transfections were performed by a chemical agent (Jet PEI). Transfected cells were distributed in 384-well plates and were allowed to recover for 24 h. The culture medium was then removed and replaced by fresh medium containing the compounds to be tested (variable concentration in 0.5% DMSO). After an overnight incubation, luciferase expression was measured by adding SteadyGlo according to the manufacturer's instructions (Promega). Fenofibric acid at  $10^{-5}$  M (PPAR $\alpha$ ), GW501516 at  $10^{-8}$  M (PPAR $\delta$ ), and rosiglitazone at  $10^{-6}$  M (PPAR $\gamma$ ) were used as references. Results were expressed as fold induction compared to basal

level or as percentage activity compared to references taken as 100%. Calculation and plate validation from run to run were done using the software Assay Explorer (MDL). Serial dilutions of compounds (final concentration ranging from 30 to 0.001  $\mu$ M) were tested in triplicate on an automated screening core-system from Beckman or Caliper. The EC<sub>50</sub> calculation was done using Assay Explorer (MDL) and was determined simultaneously on human and mouse PPAR $\alpha$ / $\delta$ / $\gamma$ .

**In Vitro Caco2 Permeability Assessment.** Compounds were tested at 10  $\mu$ M in a 96-well permeable plate seeded with Caco-2 cells. The medium was the same in apical and basolateral sides: Hanks' Balanced Salt Solution (HBSS) + 5 mM Hepes + bovine serum albumin 1%, pH 7.4. The assay was performed with a robotic platform (Caliper-PerkinElmer system). After incubation for 2 h, the concentrations of tested compound was measured in both sides by LC/MS/MS (API4000 Qtrap, AB Sciex). Permeability in both directions (apical to basolateral and basolateral to apical) was assessed to determine the efflux ratio.

**Beta-Oxidation Assays.** The functional PPAR $\alpha$  and PPAR $\delta$  activity was determined in two cell lines, HuH7 (human liver hepatoma cells, JCRB 0403) and C2C12 (mouse muscle cells differentiated into myotubes, ATCC CRL-1772) as a measurement of oleate beta-oxidation.

Cells were seeded into Petri dishes with a central well and incubated in DMEM medium at 37 °C. Compounds were added in DMSO (0.1% final concentration) at, at least, three different concentrations for 48 h. Two hours before the end of the incubation period, albumin-bound  $^{14}C$ -oleate was added in the cell medium culture. The reaction was stopped by addition of a 40% perchloric acid solution to remove excess  $^{14}C$ -oleate in the medium.

Given off CO<sub>2</sub> was trapped by KOH in the central well after sealing of the dishes, for 90 min, at room temperature and then counted.

Compounds were tested in triplicate for each concentration. Data are expressed as % of variation vs GW501516 used as reference compound at 0.1  $\mu$ M.

**Gene Expression Analysis.** After thawing, human preadipocytes (Biopredic) were amplified for 7 days in medium supplemented with growth factors (DMEM/F12 + SupplementPack/Preadipocyte C-39427 from PromoCell). Then, differentiation was induced by incubation in adipocyte medium (AM-1, ZenBio) supplemented with 0.2 mM of IBMX for 3 days with or without compound. In each culture plate, rosiglitazone at  $10^{-6}$  M was used as reference, and DMSO 0.1% as control.

Serial dilutions of compounds in the culture medium were tested in triplicate (0.1% DMSO final concentration). After 3 days, cells were rinsed three times in PBS and then immediately lysed.

Total RNA was extracted, quantified, and reverse transcribed. An aliquot of cDNA was used to perform a Sybr green real Time PCR. The specific primer sets were designed using the RefSeq sequence (NCBI <http://www.ncbi.nlm.nih.gov/RefSeq/>) on Beacon Designer 4 software (Premier Biosoft). The primer sequences of the analyzed different genes were as follows: ap2 (NM\_001442), forward 5'-ACAGGAAAGTCAAGAGCACCAT-3', reverse 5'-GCATT-CCACCACCAGTTTATC-3'; Adiponectin (NM\_004797), forward 5'-GGCTATGCTCTTCACCTATG-3', reverse 5'-ACGCTCTCCT-TCCCCATAC-3'; RPLP0 (NM\_001002), forward 5'-GCCAATAAGGTGCCAGCTGCT-3', reverse 5'-ATGGTGCCCTGGAGATT-TT-3'. ap2 and Adiponectin mRNA relative amounts were obtained from a standard curve done with increasing amount of cDNA and normalized from those of RPLP0 used as the housekeeping gene. Quantifications were done in triplicate. Results were expressed as percentages of the rosiglitazone ( $10^{-6}$  M) response. Means and standard deviations were calculated.

**In Vivo Studies.** The animals were housed in groups of 3–10 in polypropylene cages (floor area = 1032 cm<sup>2</sup>) under standard conditions: room temperature (22  $\pm$  2 °C), hygrometry (55  $\pm$  10%), light/dark cycle (12 h/12 h), air replacement (15–20 volumes/h), and water and food (SDS, RM1) ad libitum. Mice were allowed to habituate for at least 5 days prior to experimentation. Mice were numbered by marking their tail using indelible markers

The study was conducted under EU animal welfare regulation for animal use in experimentation (European Directive 2010/63/EEC).

This experimental protocol was submitted for approval by the Inventiva Ethical Committee “Comité de réflexion Ethique en Expérimentation Animale” (CR2EA) (registered by the “Ministère de l’Enseignement Supérieur et de la Recherche” under No. 104). All the procedures described below were reviewed and approved by the Inventiva ethics committee. Inventiva is a company that is AAALAC fully accredited.

**In Vivo Pharmacokinetic Studies.** The dosing was single q.d., as a suspension in methylcellulose 400 cps 1%/poloxamer 188 0.1%/water. Blood was collected up to 72 h after administration with no predose sampling. Three animals per sampling time were used (sparse sampling). Blood was collected in tubes containing evaporated lithium heparinate and centrifuged without delay at about 4 °C for ca. 10 min to obtain plasma. Plasma was then acidified with 4 N HCOOH (4%; v/v), i.e., 4  $\mu$ L of the acidic solution for 96  $\mu$ L of plasma, mixed, and then divided in two aliquots of 70  $\mu$ L when possible. All samples were stored at –20 °C until bioanalysis. Pharmacokinetic parameters were estimated by noncompartmental analysis.

**In Vivo Animal Model of Diabetic Dyslipidemia: db/db Mice.** Homozygous C57BL/Ks-db male mice (db/db mice), 11 to 13 weeks old at the start of the studies, are divided up into groups of 9–10 animals. The compounds are administered orally once a day for 5 or 10 days. One group of mice receives the vehicle only (0.5 or 1% methyl cellulose solution). A blood sample is taken from the retro-orbital sinus before treatment and 4 h after the last gavage. After centrifugation, the serum is collected, and the triglycerides and glucose levels are measured using a multiparameter analyzer with commercial kits. The results are expressed in % variation on the final day relative to the control group.

**In Vivo Animal Model of Fibrosis: CCl<sub>4</sub> C57Bl6/J Mice.** C57Bl6/J mice (6 weeks of age; ~25 g) received twice a week during 3 weeks 100  $\mu$ L i.p. of either sunflower seed oil or carbon tetrachlorure (CCl<sub>4</sub>) at a dose of 3.5 mL/kg diluted in sunflower seed oil. Compound **5** (3, 10, or 30 mg/kg) was administered per os once daily on top of CCl<sub>4</sub> during 3 weeks (*n* = 8 per group). Blood and liver were collected for RNA, protein, and histological analysis. Triglycerides and adiponectin level were evaluated in the plasma. Liver collagen was evaluated by PicroSirius Red (PSR) staining. For analysis of the PSR stained sections, the NIS-Elements software from Nikon was used.

The sections were scanned and a threshold defined by a certain intensity of PSR staining was applied on the liver section. The numerical values corresponding to the area of stained tissue define by the threshold were analyzed. This analysis gave rise to a percentage of collagen deposition within the cortex area. This analysis was performed in blinded manner.

**In Vivo Safety Model: Sprague–Dawley Rats.** Sprague–Dawley rats (6 weeks of age) were fed with a standard pellet diet or a diet supplemented with compounds at a low or a high dose. Tested compounds were **5** (100 and 1000 mg/kg), **1a** (3 and 30 mg/kg), **3a** (10 and 100 mg/kg), and **3b** (1 and 10 mg/kg). Plasma volume was measured by Evans blue dye dilution. Briefly, conscious animals were briefly restrained in a commercial restrainer for tail vein injection of 1 mg of Evans blue dye (200  $\mu$ L in saline). After 10 min, 0.5 mL of blood was withdrawn from orbital sinus under light anesthesia. A small amount was withdrawn into two hematocrit capillaries and centrifuged for 5 min at 12,000g to measure hematocrit. The remainder of the sample was centrifuged for 10 min at 3500g, and dye concentration was determined in the plasma. The absorbance measured at 620 nm was compared with a standard curve generated by using a pool of blood from three untreated rats.

**Cofactor Recruitment Assays.** Recombinant GST-tagged PPAR $\gamma$  protein was expressed in *E. coli* and purified via affinity chromatography. N-Terminal biotinylated peptide (see Table 1) was chemically synthesized, and Lumi4-Tb Cryptate conjugated anti GST Ab serves as fluorescent donor and comes from CisBio (61GSTTLA/B). Streptavidin-XL665 serves as fluorescent acceptor and is purchased from CisBio (610SAXLA/B).

These four main reagents were mixed in a Tris buffer, together with different compound concentrations and after 1 h incubation at room temperature, the time-resolved FRET signal is measured in a VictorWallac4 with 320 nm as excitation and 665 and 615 nm as emission wavelengths.

The GST-tagged PPAR $\gamma$  fragment (aa 202–505 of P37231) protein binds to the antiGST-Tb antibody. The biotinylated peptide binds to the SA-XL665 complex.

The nuclear receptor-Tb complex and the peptide-APC complex do bind to each other to a different extent. The titration of an agonistic

Peptide name	ID	Sequence
CBP (58–80)	NP_004371	NH2 - NLVPDAASKHKQLSELLRGGSGS - COOH
D22 peptide	artificial	NH2 - LPYEGSLLLKLLRAPVEEV - COOH
DAX1 (132–156)	NP_000466	NH2 - CCFCEGDHPRQGSILYSLLTSSKQT - COOH
LCOR (39–63)	NP_115816	NH2 - VTTSPATAATTQNPVLSKLLMADQDS - COOH
NCoA3 (607–631)	NP_858045	NH2 - ENQRGPLESKGHKLLQLLTCSDD - COOH
NCoA3 (671–695)	NP_858045	NH2 - SNMHGSLLEKHKRILHKLQNGNSP - COOH
NCoA3 (724–748)	NP_858045	NH2 - QEQLSPKKKENNALLRYLLDRDDPS - COOH
PERC NR1 (145–168)	NP_573570	NH2 - APAPEVDELSLLQKLLATSPTS - COOH
PERC NR2 (332–354)	NP_573570	NH2 - HSKASWAEFSILRELLAQDVLC - COOH
PGC1 (196–221)	NP_037393	NH2 - CQQQKPQRRPCSELLKYLTNTDDPP - COOH
PNRC1 (302–327)	NP_006804	NH2 - GSTVENSQNRELMVHLKTLKLVQT - COOH
RAP250 (873–897)	NP_054790	NH2 - GFPVNKDVTLSPLLVNLLQSDISA - COOH
RIP140 (118–143)	P48552	NH2 - MVDSPVKGKQDSTLLASLLQSFSSR - COOH
RIP140 (366–390)	P48552	NH2 - LERNNIKQAANNLSLLHLKLSQTIP - COOH
RIP140 (805–829)	P48552	NH2 - PVSPQDFSFSKNGLLSRLLRQNDQS - COOH
RIP140 (922–946)	P48552	NH2 - EHRWARESKSFNVLKQLLSENCV - COOH
SHP (7–31)	NP_068804	NH2 - GACFCQGAASRPAILYALLSSSLKA - COOH
SRC1 (104–128)	NP_068804	NH2 - AVTFEVAEAPVPSILKKILLEPSS - COOH
SRC1 (619–643)	NP_003734	NH2 - RLSDGDSKYSQTSKHLVQLLTTTAEQ - COOH
SRC1 (676–700)	NP_003734	NH2 - CPSSHSLTERHKILHRLQEGSPS - COOH
SRC1 (735–759)	NP_003734	NH2 - LDASKKESKDHQLRLRYLLDKDEKD - COOH
TIF2 (628–651)	NP_006531	NH2 - GQSRLLHDSKGQTKLLQLLTTSKSDQ - COOH
TIF2 (676–700)	NP_006531	NH2 - GSTHGTSLKEKHILHRLQDSSSP - COOH
TIF2 (731–755)	Q15596	NH2 - KQEPVSPKKKENALLRYLLDKDDTK - COOH
TRAP220 (590–614)	NP_004765	NH2 - GHGEDFSKVSQNPILTSLQLQTGNG - COOH
NCOR-ID1 (2253–2277)	NP_006302	NH2 - SFADPASNLGLEDIIRKALMGSFDD - COOH
SMRT-ID1 (2339–2363)	NP_006303	NH2 - VQEHASTNMGLEAIRKALMGKYDQ - COOH



ligand (see Table 2) and its binding to the respective nuclear receptor leads to an increased binding of the nuclear receptor to the coactivator peptide (all used peptides, except for NCOR-ID1 and SMRT-ID1 derived peptides), resulting in an increasing FRET signal. The two corepressor peptides (NCOR-ID1, SMRT-ID1) are displaced for the nuclear receptor upon binding of an agonist.

Assays were done in a final volume of 25  $\mu$ L in a 384-well plate. The compounds were dissolved in DMSO as vehicle. The final DMSO concentration in all experiments is 1%. All test compounds were diluted in 3-fold steps. All experiments were done in duplicate.

## ■ ASSOCIATED CONTENT

### ■ Supporting Information

The Supporting Information is available free of charge on the ACS Publications website at DOI: 10.1021/acs.jmedchem.7b01285.

Molecular Formula Strings (CSV)

### Accession Codes

Atomic coordinates and structure factors for the crystal structures of PPAR $\gamma$  with compound 5 can be accessed using PDB code 6ENQ.

## ■ AUTHOR INFORMATION

### Corresponding Author

\*Tel: +33 3 80 44 75 27. E-mail: [benaissa.boubia@inventivapharma.com](mailto:benaissa.boubia@inventivapharma.com).

### ORCID

Benaïssa Boubia: 0000-0001-6271-6440

Jérôme Amaudrut: 0000-0003-0498-4089

### Notes

The authors declare no competing financial interest.

## ■ ACKNOWLEDGMENTS

We thank Frederic Bell, Luc Spitzer, Florence Chirade, Annick Reboul, and Didier Bressac for their contribution to this work. We thank Fabrice Ciesielski and Mireille Tallandier for fruitful discussions and technical support.

## ■ ABBREVIATIONS

aP2, adipocyte protein 2; AUCinf, area under the concentration–time curve extrapolated to infinity; C2C12, mouse myoblast cell line; C57Bl6, common inbred strain of laboratory mouse; Caco-2, human Caucasian colon adenocarcinoma; CCl<sub>4</sub>, carbon tetrachloride; CF<sub>3</sub>, trifluoromethyl; CH<sub>2</sub>Cl<sub>2</sub>, dichloroethane; C<sub>max</sub>, maximum (or peak) serum concentration that a drug achieves in a specified compartment; Cu(OAc)<sub>2</sub>, copper acetate; CuI, copper iodide; COS-7, CV-1 (simian from African green monkey) in origin, and carrying the SV40 genetic material; db/db mouse model, mice used as spontaneous type 2 diabetic animal model; DMAP, dimethylaminopyridine; DMF, dimethylformamide; EC<sub>50</sub>, half maximal effective concentration; E<sub>max</sub>, maximum efficacy; FFA, free fatty acids; Et<sub>3</sub>N, diethylamine; Gal-4, galactose-responsive transcription factor (*Saccharomyces cerevisiae* S288C); HSC, hepatic stellate cells; HTS, high throughput screening; HuH7, human hepatoma cell line; KOH, potassium hydroxide; LBD, ligand binding domain; LBP, ligand binding pockets; LCOR, ligand-dependent corepressor; LiOH, lithium hydroxide; NCoA3, nuclear receptor coactivator 3; NCOR-ID1, nuclear receptor corepressor 1; NaH, sodium hydride; NASH, nonalcoholic steatohepatitis; PDB, protein database; Pd(PPh<sub>3</sub>)<sub>2</sub>Cl<sub>2</sub>, bis(triphenylphosphine)palladium(II) dichloride; PGC1 $\alpha$ , PPAR $\gamma$  coactivator-1 $\alpha$ ; PNRC1, proline-rich nuclear receptor coactivator 1; PPAR, peroxisome

proliferator-activated receptor; PSR, picrosirius red; RIP140, receptor interacting protein 140; SAR, in vitro structure–activity relationship; SMRT, silencing mediator of retinoic acid and thyroid hormone receptor; SPPARM, selective peroxisome proliferator activated receptor modulator; SRC-1, steroid receptor coactivator 1; TFA, trifluoroacetic acid; THF, tetrahydrofuran; T<sub>max</sub>, amount of time that a drug is present at the maximum concentration in serum; TR-FRET, time-resolved fluorescence energy transfer

## ■ REFERENCES

- (1) Vanni, E.; Bugianesi, E.; Kotronen, A.; De Minicis, S.; Yki-Järvinen, H.; Svegliati-Baroni, G. From the metabolic syndrome to NAFLD or vice versa? *Dig. Liver Dis.* **2010**, 42 (5), 320–330.
- (2) Harrison, S.; Torgerson, S.; Hayashi, P. H. The natural history of nonalcoholic fatty liver disease: a clinical histopathological study. *Am. J. Gastroenterol.* **2003**, 98 (9), 2042–2047.
- (3) Ekstedt, M.; Hagström, H.; Nasr, P.; Fredrikson, M.; Stål, P.; Kechagias, S.; Hultcrantz, R. Fibrosis stage is the strongest predictor for disease-specific mortality in NAFLD after up to 33 years of follow-up. *Hepatology (Hoboken, NJ, U. S.)* **2015**, 61 (5), 1547–1554.
- (4) Willson, T. M.; Brown, P. J.; Sternbach, D. D.; Henke, B. R. The PPARs: From orphan receptors to drug discovery. *J. Med. Chem.* **2000**, 43, 527–550.
- (5) Tyagi, S.; Gupta, P.; Singh Saini, A.; Kaushal, C.; Sharma, S. The peroxisome proliferator-activated receptor: A family of nuclear receptors role in various diseases. *J. Adv. Pharm. Technol. Res.* **2011**, 2, 236–240.
- (6) Peters, J. M.; Shah, Y. M.; Gonzalez, F. J. The role of peroxisome proliferator-activated receptors in carcinogenesis and chemoprevention. *Nat. Rev. Cancer* **2012**, 12, 181–195.
- (7) Shearer, B. G.; Hoekstra, W. J. Recent advances in peroxisome proliferator-activated receptor science. *Curr. Med. Chem.* **2003**, 10, 267–280.
- (8) Campbell, I. W. The clinical significance of PPAR gamma agonism. *Curr. Mol. Med.* **2005**, 5, 349–363.
- (9) Stuart, K.; Hartland, A.; Bhartia, M.; Ramachandran, S. Drugs and the peroxisome proliferator activated receptors. *Front. Clin. Drug Res.: Diabetes Obes.* **2014**, 1, 149–210.
- (10) Wright, M. B.; Bortolini, M.; Tadayyon, M.; Bopst, M. Challenges and opportunities in development of PPAR agonists. *Mol. Endocrinol.* **2014**, 28 (11), 1756–1768.
- (11) Poulsen, L. la C.; Siersbæk, M.; Mandrup, S. PPARs: Fatty acid sensors controlling metabolism. *Semin. Cell Dev. Biol.* **2012**, 23 (6), 631–639.
- (12) Feige, J. N.; Gelman, L.; Michalik, L.; Desvergne, B.; Wahli, W. From molecular action to physiological outputs: Peroxisome proliferator-activated receptors are nuclear receptors at the crossroads of key cellular functions. *Prog. Lipid Res.* **2006**, 45 (2), 120–159.
- (13) Lefebvre, P.; Chinetti, G.; Fruchart, J. C.; Staels, B. Sorting out the roles of PPAR in energy metabolism and vascular homeostasis. *J. Clin. Invest.* **2006**, 116 (3), 571–580.
- (14) Zambon, A.; Gervois, P.; Pauletto, P.; Fruchart, J. C.; Staels, B. Modulation of hepatic inflammatory risk markers of cardiovascular diseases by PPAR- $\alpha$  activators: clinical and experimental evidence. *Arterioscler., Thromb., Vasc. Biol.* **2006**, 26 (5), 977–986.
- (15) Lee, C.-H.; Olson, P.; Hevener, A.; Mehl, I.; Chong, L.-W.; Olefsky, J. M.; Gonzalez, F. J.; Ham, J.; Kang, H.; Peters, J. M.; Evans, R. M. PPAR $\beta/\delta$  regulates glucose metabolism and insulin sensitivity. *Proc. Natl. Acad. Sci. U. S. A.* **2006**, 103 (9), 3444–3449.
- (16) Odegaard, J. I.; Ricardo-Gonzalez, R. R.; Red Eagle, A.; Vats, D.; Morel, C. R.; Goforth, M. H.; Subramanian, V.; Mukundan, L.; Ferrante, A. W.; Chawla, A. Alternative M2 activation of kupffer cells by PPAR $\delta$  ameliorates obesity-induced insulin resistance. *Cell Metab.* **2008**, 7 (6), 496–507.
- (17) Grygiel-Górniak, B. Peroxisome proliferator-activated receptors and their ligands: nutritional and clinical implications - a review. *Nutr. J.* **2014**, 13, 17.

- (18) Lalloyer, F.; Staels, B. Fibrates, glitazones and peroxisome proliferator-activated receptors. *Arterioscler., Thromb., Vasc. Biol.* **2010**, *30* (5), 894–899.
- (19) Hazra, S.; Xiong, S.; Wang, J.; Rippe, R. A.; Krishna, V.; Chatterjee, K.; Tsukamoto, H. Peroxisome proliferator-activated receptor induces a phenotypic switch from activated to quiescent hepatic stellate cells. *J. Biol. Chem.* **2004**, *279* (12), 11392–11401.
- (20) Marra, F.; Efsen, E.; Romanelli, R. G.; Caligiuri, A.; Pastacaldi, S.; Batignani, G.; Bonacchi, A.; Caporale, R.; Laffi, G.; Pinzani, M.; Gentilini, P. Ligands of peroxisome proliferator-activated receptor  $\gamma$  modulate profibrogenic and proinflammatory actions in hepatic stellate cells. *Gastroenterology* **2000**, *119* (2), 466–478.
- (21) Fernández-Miranda, C.; Pérez-Carreras, M.; Colina, F.; López-Alonso, G.; Vargas, C.; Solís-Herruzo, J. A. A pilot trial of fenofibrate for the treatment of non-alcoholic fatty liver disease. *Dig. Liver Dis.* **2008**, *40* (3), 200–205.
- (22) Tenenbaum, A.; Motro, M.; Fisman, E. Z.; Schwammenthal, E.; Adler, Y.; Goldenberg, I.; Leor, J.; Boyko, V.; Mandelzweig, L.; Behar, S. Peroxisome proliferator-activated receptor ligand bezafibrate for prevention of type 2 diabetes mellitus in patients with coronary artery disease. *Circulation* **2004**, *109* (18), 2197–2202.
- (23) Cusi, K.; Orsak, B.; Bril, F.; Lomonaco, R.; Hecht, J.; Ortiz-Lopez, C.; Tio, F.; Hardies, J.; Darland, C.; Musi, N.; Webb, A.; Portillo-Sanchez, P. Long-Term pioglitazone treatment for patients with nonalcoholic steatohepatitis and prediabetes or type 2 diabetes mellitus: a randomized trial. *Ann. Intern. Med.* **2016**, *165* (5), 305–315.
- (24) Binet, J.; Boubia, B.; Dodey, P.; Legendre, C.; Barth, M.; Poupardin-Olivier, O. Novel Indole Compounds. Patent WO2007026097, 2007.
- (25) Hiroya, K.; Itoh, S.; Ozawa, M.; Kanamori, Y.; Sakamoto, T. Efficient construction of indole rings from 2-ethynylaniline derivatives catalysed by copper(II)salts and its application to the tandem cyclisation reactions. *Tetrahedron Lett.* **2002**, *43* (7), 1277–1280.
- (26) Edgar, A. D.; Tomkiewicz, C.; Costet, P.; Legendre, C.; Aggerbeck, M.; Bouguet, J.; Staels, B.; Guyomard, C.; Pineau, T.; Barouki, R. Fenofibrate modifies transaminase gene expression via a peroxisome proliferator activated receptor  $\alpha$ -dependent pathway. *Toxicol. Lett.* **1998**, *98*, 13–23.
- (27) Piqueras, L.; Reynolds, A. R.; Hodivala-Dilke, K. M.; Alfranca, A.; Redondo, J. M.; Hatae, T.; Tanabe, T.; Warner, T. D.; Bishop-Bailey, D. Activation of PPAR $\beta$ /delta induces endothelial cell proliferation and angiogenesis. *Arterioscler., Thromb., Vasc. Biol.* **2007**, *27* (1), 63–69.
- (28) Kobayashi, K.; Forte, T. M.; Taniguchi, S.; Ishida, B. Y.; Oka, K.; Chan, L. The *db/db* mouse, a model for diabetic dyslipidemia: molecular characterization and effects of western diet feeding. *Metab., Clin. Exp.* **2000**, *49* (1), 22–31.
- (29) Wettstein, G.; Luccarini, J. M.; Poekes, L.; Faye, P.; Kupkowsky, F.; Adarbes, V.; Defrene, E.; Estivalet, C.; Gawronski, X.; Jantzen, I.; Philippot, A.; Tessier, J.; Tuyaa-Boustugue, P.; Oakley, F.; Mann, D. A.; Leclercq, I.; Francque, S.; Konstantinova, I.; Broqua, P.; Junien, J. L. The new-generation pan-peroxisome proliferator-activated receptor agonist IVA337 protects the liver from metabolic disorders and fibrosis. *Hepatology Communications* **2017**, *6* (1), 524–537.
- (30) Li, Y.; Zhulun Wang, Z.; Furukawa, N.; Escaron, P.; Jennifer Weismann, J.; Lee, G.; Lindstrom, M.; Liu, J.; Liu, X.; Xu, H.; Olga Plotnikova, O.; Vidya Prasad, V.; Walker, N.; Learned, R. M.; Chen, J. L. T2384, a Novel antidiabetic agent with unique peroxisome proliferator-activated receptor  $\gamma$  binding properties. *J. Biol. Chem.* **2008**, *283* (14), 9168–9176.
- (31) Lin, C. H.; Peng, Y. H.; Coumar, M. S.; Chittimalla, S. K.; Liao, C. C.; Lyn, P. C.; Huang, C. C.; Lien, T. W.; Lin, W. H.; Hsu, J. T. A.; Cheng, J. H.; Chen, X.; Wu, J. S.; Chao, Y. S.; Lee, H. J.; Juo, C. G.; Wu, S. Y.; Hsieh, H. P. Design and structural analysis of novel pharmacophores for potent and selective peroxisome proliferator-activated receptor  $\gamma$  agonists. *J. Med. Chem.* **2009**, *52*, 2618–2622.
- (32) Laghezza, A.; Montanari, R.; Lavecchia, A.; Piemontese, L.; Pochetti, G.; Iacobazzi, V.; Infantino, V.; Capelli, D.; De Bellis, M.; Liantonio, A.; Pierno, S.; Tortorella, P.; Conte Camerino, D.; Loiodice, F. On the metabolically active form of metaglidase: improved synthesis and investigation of its peculiar activity on peroxisome proliferator-activated receptors and skeletal muscles. *ChemMedChem* **2015**, *10*, 555–565.
- (33) Bernardes, A.; Souza, P. C. T.; Muniz, J. R. C.; Ricci, C. G.; Ayers, S. D.; Parekh, N. M.; Godoy, A. S.; Trivella, D. B. B.; Reinach, P.; Webb, P.; Skaf, M. S.; Polikarpov, I. Molecular mechanism of peroxisome proliferator-activated receptor  $\alpha$  activation by WY14643: a new mode of ligand recognition and receptor stabilization. *J. Mol. Biol.* **2013**, *425* (16), 2878–2893.
- (34) Gampe, R. T., Jr.; Montana, V. G.; Lambert, M. H.; Miller, A. B.; Bledsoe, R. K.; Milburn, M. V.; Kliewer, S. A.; Willson, T. M.; Xu, H. E. Asymmetry in the PPAR $\gamma$ /RXR $\alpha$  crystal structure reveals the molecular basis of heterodimerization among nuclear receptors. *Mol. Cell* **2000**, *5*, 545–555.
- (35) Itoh, T.; Fairall, L.; Amin, K.; Inaba, Y.; Szanto, A.; Balint, B. L.; Nagy, L.; Yamamoto, K.; Schwabe, J. W. R. Structural basis for the activation of PPAR $\gamma$  by oxidized fatty acids. *Nat. Struct. Mol. Biol.* **2008**, *15*, 924–931.
- (36) Liu, Y.; Miller, A. R. Ligands to peroxisome proliferator-activated receptors as therapeutic options for metabolic syndrome. *Drug Discovery Today: Ther. Strategies* **2005**, *2* (2), 165–169.
- (37) Liu, Z. M.; Hu, M.; Chan, P.; Tomlinson, B. Early investigational drugs targeting PPAR- $\alpha$  for the treatment of metabolic disease. *Expert Opin. Invest. Drugs* **2015**, *24* (5), 611–621.
- (38) Knouff, C.; Auwerx, J. Peroxisome proliferator-activated receptor- calls for activation in moderation: lessons from genetics and pharmacology. *Endocr. Rev.* **2004**, *25* (6), 899–918.
- (39) Dietz, M.; Mohr, P.; Kuhn, B.; Maerki, H. P.; Hartman, P.; Ruf, A.; Benz, J.; Grether, U.; Wright, M. B. Comparative molecular profiling of the PPAR $\alpha$ / $\gamma$  activator aleglitazar: PPAR selectivity, activity and interaction with cofactors. *ChemMedChem* **2012**, *7*, 1101.
- (40) Boden, G.; Homko, C.; Mozzoli, M.; Zhang, M.; Kresge, K.; Cheung, P. Combined use of rosiglitazone and fenofibrate in patients with type 2 diabetes: prevention of fluid retention. *Diabetes* **2007**, *56*, 248–255.
- (41) Smith, S. Y.; Samadfam, R.; Chouinard, L.; Awori, M.; Bénardeau, A.; Bauss, F.; Guldborg, R. E.; Sebkova, E.; Wright, M. B. Effects of pioglitazone and fenofibrate co-administration on bone biomechanics and histomorphometry in ovariectomized rats. *J. Bone Miner. Metab.* **2015**, *33* (6), 625–641.

#### ■ NOTE ADDED AFTER ASAP PUBLICATION

After this paper was published ASAP February 27, 2018, a change was made to the table in the Experimental Section. The revised version was reposted March 1, 2018.